Maternal Aggression Driven by the Transient Mobilization of a Dormant Hormone-Sensitive Circuit

Stefanos Stagkourakis[1,,¶], Paul Williams[2], Giada Spigolon[1], Shreya Khanal[1], Katharina Ziegler[1], Laura Heikkinen[1,2], Gilberto Fisone[1] and Christian Broberger[1,2,*]*

[1]Department of Neuroscience, Biomedicum B:4, Karolinska Institutet, Solnavägen 9, 171 65 Stockholm, Sweden

[2]Department of Biochemistry and Biophysics, Stockholm University, Svante Arrhenius väg 16C, 106 91 Stockholm, Sweden

[¶]Current address: Division of Biology and Biological Engineering 156-29, Tianqiao and Chrissy Chen Institute for Neuroscience, California Institute of Technology, Pasadena, CA 91125, USA

*Correspondence: stefanos.stagkourakis@caltech.edu, christian.broberger@dbb.su.se

Acknowledgments

Members of the Broberger laboratory are thanked for advice and discussion during the preparation of this manuscript, as are the many investigators who originally developed the reagents and tools that made this study possible. The authors gratefully acknowledge support by a project grant from the Knut and Alice Wallenberg Foundation (2020.0054), a European Research Council Advanced Grant (TOGETHER 101021496), a Distinguished Professor Grant from the Swedish Research Council (021-00671), funding from *Hjärnfonden* (the Swedish Brain Foundation), and internal Stockholm University funds to C.B. S.S. is a Wenner-Gren Fellow, supported by the Wenner-Gren Foundations.

Author contributions

S.S. and C.B. conceived the study and wrote the manuscript. S.S. designed, performed, and analysed experiments. P.W., G.S., G.F., and C.B. designed experiments. P.W., G.S., S.K., K.Z., and L.H. performed experiments. All authors reviewed the manuscript.

Competing interests

The authors declare no competing financial interests.

Graphical abstract

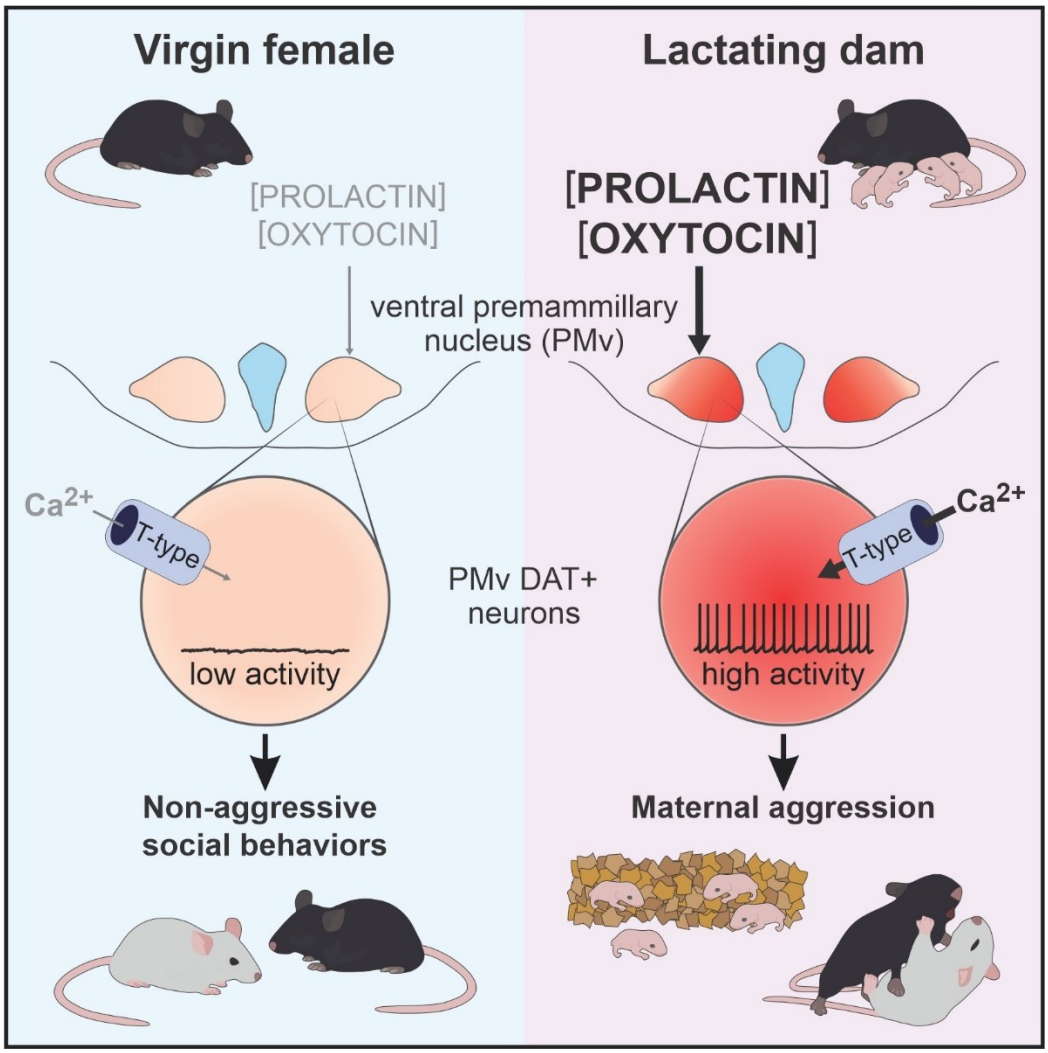

In Brief

Maternal hormones activate an otherwise quiescent population of hypothalamic neurons, which are required for the transient expression of aggression during the nursing period.

Highlights

- Quiescent PMv^{DAT} neurons in female mice become hyperexcitable in lactating dams.
- Manipulation of PMv^{DAT} cell activity bidirectionally regulates maternal aggression.
- The maternal hormones prolactin and oxytocin excite PMv^{DAT} cells.
- Activation of PMv^{DAT} neurons impairs non-aggression maternal care behaviour.

Summary

Aggression, a sexually dimorphic behaviour, is prevalent in males and typically absent in virgin females. Following parturition, however, the transient expression of aggression in adult female mice protects pups from predators and infanticide. While maternal hormones are known to elicit nursing, their potential role in maternal aggression remains elusive. Here, we show in mice that a molecularly defined subset of ventral premammillary (PMv^{DAT}) neurons, instrumental for intermale aggression, switch from quiescence to a hyperexcitable state during lactation. We identify that the maternal hormones prolactin and oxytocin excite these cells through actions on T-type Ca^{2+} channels. Optogenetic manipulation or genetic ablation of PMv^{DAT} neurons profoundly affects maternal aggression, while activation of these neurons impairs the expression of non-aggression-related maternal behaviours. This work identifies a monomorphic neural substrate that incorporates hormonal cues to enable the transient expression of a dormant behavioural program in adult females.

Introduction

Aggression is a near-ubiquitous adaptive behaviour in animals and man that serves multiple purposes and takes several forms, depending on agent and context[1-8]. Intermale aggression is arguably the best studied form of aggression found in nature, serving to establish social hierarchy and, consequently, access to resources and mating opportunities. In contrast, aggressive encounters in female mammals are typically absent, with some notable exceptions[9-11]. Female interactions with conspecifics, however, change dramatically after pregnancy and parturition, when lactating dams typically exhibit profound aggressive behaviour towards both males and females of the same species[12]. Indeed, maternal aggression is as indelible as other components of maternal behaviour, such as nursing and nest-building. This dramatic – yet reversible[13] – phenotypical metamorphosis powerfully exemplifies a neurobiological challenge, specifically: How does the brain reconfigure to transiently enable the expression of a behaviour that is otherwise outside of the animal's repertoire? The brain loci and mechanisms underlying maternal aggression are largely unknown and the signals that drive this transition, alongside their site of action, remain ambiguous. Importantly, it is not well understood if the neural modules that lead to the expression of aggression are shared between the two sexes, or exhibit sexual dimorphism. Finally, it is unknown if brain nodes that elicit certain maternal behaviours facilitate or impair the expression of other behaviours typical of the mother.

Here we address the above questions by focusing on the ventral premammillary nucleus (PMv), which is coextensive with the caudal two-thirds of the classically defined "hypothalamic attack area" [14], and which has been implicated in social behaviour[15-17] and intermale aggression[18-21]. This nucleus receives dense innervation from areas associated with sensory processing[22], and projects[23] to nuclei implicated in social behaviour[24-27], aggression[19,28-31], and reward[20,32-35]. Within the PMv, a subset of glutamatergic cells that express the dopamine transporter gene (PMv^{DAT} neurons) have been specifically implicated in male agonistic behaviours[18,20,21].

Here we identify PMv^{DAT} cells as quiescent in the virgin female mouse brain, with a dramatic switch in their excitability during motherhood – excited by the hormones that surge during nursing and which facilitate the expression of maternal care. Specifically, prolactin (Prl) triggers excitatory pre- and post-synaptic changes, an effect mimicked by another maternal hormone, oxytocin (OT). Optogenetic manipulation and deletion of these neurons revealed that their activity is instrumental in the expression of maternal aggression. Finally, activation of PMv^{DAT} neurons during a maternal care paradigm impairs the expression of pup retrieval and nursing, suggestive of a specialised role of PMv cells in prioritising a distinct behavioural expression at the expense of others.

The present study suggests how the transient sex-specific expression of an adaptive behaviour can result from state-dependent reversal of neuronal excitability.

105 # Results

106 **Low *vs* high baseline activity of PMv^{DAT} cells in virgin *vs* postpartum females**

107 While maternal aggression is widespread in the animal kingdom, recent studies suggest
108 substantial inter-individual variability in the expression of aggressive behaviour[36,37]. Furthermore, a
109 number of variables impact on the expression of maternal aggression, including litter size[38], pup
110 presence[39], and the intruder's sex[40] and behaviour[41]. To control for these factors, we used a three
111 consecutive day (p3-p5) resident-intruder (RI) paradigm to screen lactating dams for aggressive
112 behaviour, using C57 or BALB/c juvenile virgin female mice (p40-50) as intruders and restricting litter
113 size to four to six pups *post partum*. Under this paradigm, 42% of multiparous lactating dams
114 expressed maternal aggression (Figure 1A), with increased duration and decreased latency upon
115 repeated experience in aggressive encounters (Figure 1B), similar to what is observed in intermale
116 aggression using the same paradigm[20,35,42] and in proportions in agreement with earlier descriptions
117 of maternal aggression[43].

118 PMv neurons have been reported to activate in conjunction with an aggressive encounter in
119 lactating rat dams[17]. To determine if this includes the PMv^{DAT} neurons, we examined c-Fos
120 immunoreactivity. Both the total number of c-Fos^{+} neurons, and the proportion of DAT^{+} cells containing
121 c-Fos immunoreactivity, were increased following the expression of maternal aggression (Figure 1C,
122 D, Table S1).

123 A subpopulation of male laboratory rodents consistently present as non-aggressive in the RI
124 paradigm[20,35,42]. Strikingly, PMv^{DAT} neurons in male non-aggressor mice are significantly less
125 electrically excitable than in aggressors (*21*). This observation prompted the question of whether a
126 similar phenotype-correlated electrical profile can be seen in lactating (aggressive) mice *vs*. virgin
127 female mice[44,45], which are non-aggressive. Brain slice whole-cell patch-clamp recordings were
128 performed on PMv^{DAT} cells, which were *post-hoc* reconstructed (Figure 1E, F). Notably, PMv^{DAT} cells
129 from lactating dams were in a hyperexcited state compared to those from virgin females (Figure 1G),
130 exhibiting significantly higher firing frequency (Figure 1H, Table S1) and a more depolarised resting
131 membrane potential (Figure 1I, Table S1).

132

133

134 **Bidirectional control of maternal aggression through PMv^{DAT} neurons**

135 Having established that PMv^{DAT} neurons are in a hyperexcitable state in lactating dams compared
136 to the non-aggressive virgin female mouse, we next performed activation, inactivation and deletion of
137 these cells in order to investigate the effect of such manipulations *in vivo* on maternal aggression.
138 Genetic modifications were introduced into PMv^{DAT} neurons by stereotactic injection of Cre-dependent
139 constructs within an AAV vector.

140 PMv^{DAT} neurons in lactating dams were transduced with channelrhodopsin-2 (ChR2, Figure 2A)
141 and behaviour was recorded in RI trials in the presence of male and female conspecifics (Figure 2B).
142 Minimal control-condition maternal aggression was attained in this experimental design by introducing
143 an adult intruder (typically five months old and 30-35 grams in weight), in agreement with previous
144 literature[46,47], and baseline behaviour was characterised by close investigation, but rare expressions
145 of aggression (Figure 2C). Optogenetic stimulation of PMv^{DAT} cells resulted in significantly prolonged
146 attack bouts appearing within seconds of initiation of photostimulation (Figure 2C-E, Video S1, Table
147 S1).
148 To determine the behavioural effect of inhibition of the PMv^{DAT} population, these cells in lactating
149 dams were transduced with halorhodopsin-3 (eNpHR3, Figure 2F) and juvenile female intruders were
150 used to facilitate high levels of maternal aggression in baseline conditions[40,47] (Figure 2G). Indeed,
151 under these control conditions, lactating dams frequently engaged in sustained attacks. However,
152 optogenetic inhibition of their PMv^{DAT} neurons was followed by decreased attack bout duration and
153 delayed initiation of subsequent attack episodes (Figure 2H-J, Table S1).
154 Lastly, genetic deletion of the PMv^{DAT} neurons in lactating dams – sparing neighbouring DAT
155 neuron populations (Figure S1A, B and Table S1) – and subsequent RI testing (Figure 2K, L)
156 dramatically decreased the attack frequency and duration and increased latency to attack (Figure 2M-
157 O, Table S1), in agreement with an earlier report applying non-specific excitotoxic PMv lesions[17].
158 Together, these experiments establish a causal role for PMv^{DAT} neurons in the expression of maternal
159 aggression.
160
161 **Maternal hormones excite PMv^{DAT} neurons**
162 Endocrine hallmarks of the *post partum* female include a surge in the serum levels of specific
163 hormones[48-52]. Among these hormones, the most well-documented maternal functions are served by
164 Prl[53], which rises in late pregnancy and remains elevated after birth in rodents[54-56], facilitating maternal
165 pup care behaviour and offspring survival[57-59]. Similar dynamics are shown by OT, which plays a
166 parallel and complementary role in the mother's care for offspring [60-63]. We next explored if these
167 maternal hormones can affect the activity of PMv^{DAT} neurons that the data above implicate in
168 puerperal aggression.
169 Serum levels of Prl were found ten-fold higher in lactating mouse dams compared to virgin females
170 at any point across the estrous cycle (Figure 3A, Table S1), confirming earlier literature[64]. We next
171 determined if this difference in circulating Prl corresponds to differential Prl receptor (Prl-R) activation
172 in the PMv of virgin *vs* lactating female mice. Indeed, phosphorylation of the Signal Transducer and
173 Activator of Transcription 5 (pSTAT5), a key sensitive downstream mediator of Prl-R activation[65-76],
174 was significantly elevated in PMv^{DAT} neurons in lactating females (Figure 3B-D, Table S1). These
175 findings prompted the question of whether PMv^{DAT} cells can be directly modulated by Prl.

176 Application of Prl to PMv^{DAT} neurons during *in vitro* patch clamp recordings yielded several
177 electrophysiological changes, which can increase the excitability and output of these cells. Firstly, a
178 prominent and reversible depolarisation, paralleled by increased discharge frequency, was seen
179 (Figure 3E, Table S1), similar to observations from genetically unidentified PMv neurons[77]. Secondly,
180 action potential duration was significantly prolonged (Figure 3F, Table S1), levels that can elicit an
181 increase of neurotransmitter release by an order of magnitude[78]. Thirdly, the capacity for, and
182 strength of, post-inhibitory rebound were augmented (Figure 3G, Table S1), key features of PMv^{DAT}
183 neurons and implicated in their propensity for regenerative discharge[20]. The post-synaptic Prl-induced
184 current in PMv^{DAT} cells consisted of a low- and a high-voltage component (Figure 3H, Table S1).
185 Application of the selective T-type low-threshold Ca^{2+} current blocker, ML218, abolished the low-
186 voltage component (Figure 3I, Table S1). Lastly, we tested whether blocking the T-type Ca^{2+} channels
187 impaired the post-inhibitory rebound, and the Prl induced potentiation of rebound excitation. Indeed,
188 ML218 abolished the post-inhibitory rebound current and effect of Prl at below firing threshold
189 membrane potential (data not shown).
190 Interestingly, the application of Prl also affected synaptic input into PMv^{DAT} neurons, with an
191 increase of both spontaneous excitatory (Figure 3J, Table S1) and inhibitory post-synaptic currents
192 (data not shown). A likely source of the increased excitatory synaptic currents is recurrent axon
193 collaterals, as the glutamatergic PMv^{DAT} population is densely interconnected[20]. These data reveal a
194 wide repertoire of Prl actions on the membrane properties of PMv^{DAT} neurons that together converge
195 to increase excitability.
196 Oxytocin, beyond its role in milk ejection[79-81], is most commonly discussed as an agent of maternal
197 care and social bonding[82,83]. Previous studies have, however, also correlated increased serum OT
198 levels to maternal aggression[37,84,85]. Yet, a cellular mechanism for how OT might promote attack
199 behaviour in dams remains elusive. Immunofluorescence staining of the PMv identified close
200 appositions between OT positive fibers and PMv^{DAT} cell somata (Figure 3K). This finding, and the
201 presence of OT receptors (OT-R's) in the PMv[86], led us to evaluate the responsiveness of PMv^{DAT}
202 neurons to OT. Application of OT yielded a reversible depolarisation of PMv^{DAT} neurons (Figure 3L,
203 Table S1), similar to the effect of Prl (as above), as did application of the selective OT-R agonist,
204 TGOT[87,88] (Figure 3M, Table S1). However, the effect of OT persisted in the presence of an OT-R
205 antagonist (vasotocin [d(CH2)$_5^1$, Tyr(Me)^2, Thr^4, Orn^8, des-Gly NH_2^9]), indicating that vasopressin
206 receptors [89-94] may contribute to the peptide's action on PMv^{DAT} neurons (Figure 3M, Table S1). The
207 OT effect depended on a post-synaptic depolarisation, composed of low- and high-voltage
208 components similar to the Prl-induced current (Figure 3N, Table S1).
209 To investigate whether maternal hormones acting in the PMv are sufficient to trigger aggression
210 in an inherently non-aggressive female, we performed a 28-day localised application of Prl, OT, or
211 both peptide hormones (co-administration) unilaterally into the nucleus of virgin female adult mice.
212 Two weeks after implantation we performed a panel of tests, to investigate changes in aggressive

213 and/or alloparental behaviour, as well as other behavioural features (Figure S2A). No attacks or
214 changes in the degree of close investigation were observed in the RI test (Figure S2B and Table S1).
215 Notably, however, local co-administration of maternal hormones in the PMv decreased sociability in
216 the group (Figure S2C, Table S1) and, importantly, impaired alloparenting (Figure S2D, Table S1).
217 Modest changes in locomotion, but not anxiety parameters, were identified (Figure S2E-F, Table S1).
218 Together these experiments indicate that PMv-targetted application of maternal hormones in non-
219 lactating females does not lead to the expression of aggression, suggestive of necessary upstream
220 and/or downstream changes implemented in the brains of lactating dams, but does decrease
221 sociability and pup retrieval performance.
222
223 **Activation of PMv^{DAT} neurons impairs maternal care**
224 Aggression in dams is part of a behavioural program that turns on at parturition and declines by
225 weaning[40,95]. This program includes a coincident initiation of pup care – such as nursing, grooming
226 and crouching - and maternal aggression, aimed to inflict injury and deter infanticidal conspecifics or
227 predators from attacking the pups[95]. In the final experiment, we tested whether pup care and maternal
228 aggression can be triggered by common anatomical substrates, such as the PMv, or whether
229 activation of defined brain loci/circuitry leads to the execution of dedicated/non-overlapping
230 behavioural programs at the expense of other behaviours.
231 To investigate this issue, we tested the effect of optogenetic activation of PMv^{DAT} neurons, in the
232 absence of an intruder, during a pup retrieval test[96,97]. The pup retrieval test was performed with
233 lactating dams expressing ChR2 or eYFP in PMv^{DAT} neurons (Figure 4A). Control (eYFP-expressing)
234 dams retrieved all pups within one minute of the task initiation during photostimulation (Figure 4B, D,
235 E, Video S2, Table S1). In contrast, photostimulated ChR2-expressing dams exhibited severely
236 impaired pup retrieval behaviour and, in many cases, failed to retrieve any pups over the maximum
237 test period of three minutes (Figure 4B-E, Video S3, Table S1). No aggression towards the pups was
238 observed in any of the trials.
239 These data suggest that activation of these neurons promotes a specialised behavioural program
240 – the one of maternal aggression – at the expense of other maternal behaviours. Thus, even in the
241 absence of a competing intruder stimulus, normal nursing behaviour is inhibited when the PMv^{DAT}
242 population is activated.
243

Discussion

Maternal aggression is a well-established adaptive behaviour across species, remarkable for its sudden onset and reversibility in adulthood[12,98]. The neuronal substrate that underlies the transient aggressive state of the dam has long remained elusive. In recent years, key elements of a brain architecture that drives intermale aggression have been identified[19,20,99-102]; some of these loci have also been implicated in the expression of aggression in females[9,101,103]. However, it cannot be automatically inferred that the same neurons drive maternal attacks, as the behaviour is manifested through distinct action patterns[37,43,101]. Importantly, a circuit-based model of maternal aggression needs to account for the transient nature of this trait.

Here we show that PMv^{DAT} neurons, a key population in orchestrating intermale aggression[21], are typically quiescent in the virgin female but undergo a dramatic shift to an active state during nursing and are required for the expression of maternal aggression. Stimulation of these cells disrupts maternal pup care, even in the absence of overt aggression. The hallmark hormonal agents of lactation, Prl and OT, can powerfully, and through multiple convergent mechanisms, trigger hyperexcitability in these cells. These findings suggest a flexible neural framework for hormonally driven generation of adaptive aggression.

Mechanisms have been explored to explain the inherent – purportedly stable – aggression and non-aggression phenotypes of male animals, and one substrate has been found in the electrical excitability of PMv^{DAT} neurons[20]. But traits do not always remain static over lifetime. The present results show that PMv^{DAT} cells are relatively hyperpolarised below firing threshold in virgin females, but enter a depolarised state of action potential discharge in nursing dams. Strikingly, this dichotomy closely mirrors the electrical properties of PMv^{DAT} neurons in phenotypically aggressive and non-aggressive males[31]. These findings provide experimental support to the concept that sexual dimorphism in aggression does not result from fundamentally different wiring of the male and female brain (see [104]). Rather, a common framework, activated by adaptive cues, may underlie situationally relevant attack behaviours in both sexes. This organization echoes the seminal demonstration that the neuronal substrate for male-like mating behaviour sequences also exist in the female mouse brain[99,101,105]. The present data expand this concept by showing not just the existence of such a “veiled circuit” for maternal aggression in the PMv, but that these neurons are also transiently mobilised when offspring needs to be defended to execute attacks until pups have left the nest. It remains to be determined if the different motor expressions of intermale and maternal aggression[37,43,101] reflect the engagement of distinct downstream motor pattern generators.

Sex steroids underlie the brain adaptations during pregnancy, but *post-partum* maternal-specific physiology and behaviour have been attributed to pup cues[106]. Physical interactions with pups trigger hormone release in the dam, which serves as the interface to the brain. This is illustrated by the lactation reflex, where suckling on the nipple triggers the release of OT and Prl from the pituitary

gland, driving milk production and ejection, respectively. In parallel, these hormones also initiate and maintain maternal care[57,107,108]. The induction of pSTAT5 in PMv^{DAT} neurons during lactation (present findings) suggests that Prl, and possibly also OT, may play a role in the excitability switch. Acutely, Prl increases discharge (by bringing them towards or beyond firing threshold), amplifies input-output ratio (by increasing action potential duration) and accelerates persistent activity (by promoting rebound bursting) in PMv^{DAT} cells. A similar increase in excitability is induced by OT, indicating a synergistic action of the two hormones. Collectively, this broad program of electrophysiological actions push PMv^{DAT} neurons into the hyperexcitable state that they exhibit in phenotypically aggressive mice ([31]; present findings). The roles of Prl and OT in maternal aggression remain poorly understood. Although these hormones are most commonly discussed in the context of reinforcing bonds between mother and child, there is also data pointing to their involvement in fighting off a potential threat to offspring[37,109-114]. A recent study proposed that Prl (acting in the ventrolateral subdivision of the ventromedial hypothalamus [VMHvl]) serves to dampen aggression[115], seemingly at odds with the model suggested by our results. However, the nucleus-specific receptor deletion that was employed in the study may obscure the cumulative effect of the hormone in the brain on behaviour. Indeed, while stimulation of PMv^{DAT} cells is a powerful inducer of attacks in the puerperal state (present data), chemogenetic activation of VMHvl Prl receptor neurons has no effect on maternal aggression[115]. Our study and Georgescu *et al's*[115] together indicate that Prl may be a powerful modulator of aggression in dams which merits further investigation. Our data further suggest that isolated action of Prl and OT in the PMv of virgin female mice is not sufficient to trigger aggression, but that additional circuit adaptations related to pregnancy and/or nursing are required to establish this behaviour in dams.

Finally, we show that stimulation of the PMv^{DAT} neurons – the same paradigm that powerfully promoted aggressive behaviour in the resident-intruder test – does not elicit pup-directed aggression but markedly impairs parental care during a pup retrieval task. These data firstly suggest (as previously shown for the same population in males[31]) that activation of PMv^{DAT} cells does not indiscriminately promote attacks against any available target, *i.e.* pups, but rather may be specific for juvenile and adult intruders. This property of context specificity distinguishes PMv^{DAT} neurons from the well-characterised VMHvl^{ESR1} cells, which drive attacks equally well towards conspecifics or inanimate objects[116]. Secondly, it is clear that PMv^{DAT} neurons do not constitute a hub for driving the full repertoire of maternal behaviours (cf.[117]). Rather, an intriguing speculation that these results invite is that parental care of offspring is actively suppressed during aggression orchestrated via the PMv^{DAT} population. Indeed, in virgin females the infusion of OT and Prl into the PMv resulted in a disruption of alloparenting (Figure S2).

The data presented here reveal how transient activation of a circuit can allow animals to reversibly access a behaviour for adaptive purposes. Our results suggest a model in which PMv^{DAT} neurons are hormonally primed into a hyperexcitable state in the dam, greatly lowering the threshold for eliciting attacks against conspecifics. With the sudden appearance of an intruder, activation of these neurons

317 may serve to prioritise attack over nursing to direct attention and resources to the most imminent
318 threat to survival.
319
320

References

1. Maestripieri, D. Costs and Benefits of Maternal Aggression in Lactating Female Rhesus Macaques. *Primates; journal of primatology* **35**, 443-453 (1994).
2. Kent, J.P. Maternal Aggression and Interindividual Distance in the Broody Hen (Gallus-Gallus). *Behav Process* **27**, 37-44 (1992).
3. Troisi, A., Damato, F.R., Carnera, A. & Trinca, L. Maternal Aggression by Lactating Group-Living Japanese Macaque Females. *Hormones and behavior* **22**, 444-452 (1988).
4. Olivier, B.*, et al.* Maternal Aggression in Rats. *Aggressive Behav* **11**, 169-169 (1985).
5. Stockman, E.R. Aggressive Experience and Maternal Aggression in the Mongolian Gerbil. *Physiology & behavior* **30**, 319-321 (1983).
6. Siegel, H.I., Giordano, A.L., Mallafre, C.M. & Rosenblatt, J.S. Maternal Aggression in Hamsters - Effects of Stage of Lactation, Presence of Pups, and Repeated Testing. *Hormones and behavior* **17**, 86-93 (1983).
7. Stjohn, R.D. & Corning, P.A. Maternal Aggression in Mice. *Behavioral biology* **9**, 635-639 (1973).
8. Figler, M.H., Blank, G.S. & Peeke, H.V.S. Maternal aggression and post-hatch care in red swamp crayfish, Procambarus clarkii (Girard): The influences of presence of offspring, fostering, and maternal molting. *Mar Freshw Behav Phy* **30**, 173-194 (1997).
9. Hashikawa, K.*, et al.* Esr1(+) cells in the ventromedial hypothalamus control female aggression. *Nat Neurosci* **20**, 1580-1590 (2017).
10. Rendon, N.M. & Demas, G.E. Bi-directional actions of dehydroepiandrosterone and aggression in female Siberian hamsters. *Journal of experimental zoology. Part A, Ecological genetics and physiology* **325**, 116-121 (2016).
11. Been, L.E., Moore, K.M., Kennedy, B.C. & Meisel, R.L. Metabotropic Glutamate Receptor and Fragile X Signaling in a Female Model of Escalated Aggression. *Biological psychiatry* **79**, 685-692 (2016).
12. Lonstein, J.S. & Gammie, S.C. Sensory, hormonal, and neural control of maternal aggression in laboratory rodents. *Neuroscience and biobehavioral reviews* **26**, 869-888 (2002).
13. Flannelly, K.J. & Flannelly, L. Time Course of Postpartum Aggression in Rats (Rattus-Norvegicus). *Journal of comparative psychology* **101**, 101-103 (1987).
14. Kruk, M.R.*, et al.* Discriminant analysis of the localization of aggression-inducing electrode placements in the hypothalamus of male rats. *Brain research* **260**, 61-79 (1983).
15. Cavalcante, J.C., Bittencourt, J.C. & Elias, C.F. Female odors stimulate CART neurons in the ventral premammillary nucleus of male rats. *Physiology & behavior* **88**, 160-166 (2006).
16. Yokosuka, M.*, et al.* Female-soiled bedding induced Fos immunoreactivity in the ventral part of the premammillary nucleus (PMv) of the male mouse. *Physiology & behavior* **68**, 257-261 (1999).
17. Motta, S.C.*, et al.* Ventral premammillary nucleus as a critical sensory relay to the maternal aggression network. *Proc Natl Acad Sci U S A* **110**, 14438-14443 (2013).
18. Soden, M.E.*, et al.* Genetic Isolation of Hypothalamic Neurons that Regulate Context-Specific Male Social Behavior. *Cell reports* **16**, 304-313 (2016).
19. Lin, D.Y.*, et al.* Functional identification of an aggression locus in the mouse hypothalamus. *Nature* **470**, 221-+ (2011).
20. Stagkourakis, S.*, et al.* A neural network for intermale aggression to establish social hierarchy. *Nature neuroscience* **21**, 834-+ (2018).
21. Chen, A.X.*, et al.* Specific Hypothalamic Neurons Required for Sensing Conspecific Male Cues Relevant to Inter-male Aggression. *Neuron* (2020).
22. Cavalcante, J.C., Bittencourt, J.C. & Elias, C.F. Distribution of the neuronal inputs to the ventral premammillary nucleus of male and female rats. *Brain research* **1582**, 77-90 (2014).
23. Canteras, N.S., Simerly, R.B. & Swanson, L.W. Projections of the Ventral Premammillary Nucleus. *Journal of Comparative Neurology* **324**, 195-212 (1992).
24. Sanchez, M.M., Aguado, F., Sancheztoscano, F. & Saphier, D. Effects of Prolonged Social-Isolation on Responses of Neurons in the Bed Nucleus of the Stria Terminalis, Preoptic Area, and Hypothalamic

Paraventricular Nucleus to Stimulation of the Medial Amygdala. *Psychoneuroendocrinology* **20**, 525-541 (1995).

25. Duque-Wilckens, N., Steinman, M., Grinevich, V. & Trainor, B. The Role of Oxytocin Neurons in the Bed Nucleus of the Stria Terminalis in Mediating Social Withdrawal. *Biological psychiatry* **81**, S44-S45 (2017).
26. Lei, K., Cushing, B.S., Musatov, S., Ogawa, S. & Kramer, K.M. Estrogen Receptor-alpha in the Bed Nucleus of the Stria Terminalis Regulates Social Affiliation in Male Prairie Voles (Microtus ochrogaster). *PloS one* **5**(2010).
27. Jasnow, A.M., Davis, M. & Huhman, K.L. Involvement of central amygdalar and bed nucleus of the stria terminalis corticotropin-releasing factor in behavioral responses to social defeat. *Behavioral neuroscience* **118**, 1052-1061 (2004).
28. Albert, D.J., Walsh, M.L., Gorzalka, B.B., Mendelson, S. & Zalys, C. Intermale Social Aggression - Suppression by Medial Preoptic Area Lesions. *Physiology & behavior* **38**, 169-173 (1986).
29. Rosenblatt, J.S., Hazelwood, S. & Poole, J. Maternal behavior in male rats: Effects of medial preoptic area lesions and presence of maternal aggression. *Hormones and behavior* **30**, 201-215 (1996).
30. Scott, N., Prigge, M., Yizhar, O. & Kimchi, T. A sexually dimorphic hypothalamic circuit controls maternal care and oxytocin secretion. *Nature* **525**, 519-+ (2015).
31. Stagkourakis, S., Perez, C.T., Hellysaz, A., Ammari, R. & Broberger, C. Network oscillation rules imposed by species-specific electrical coupling. *eLife* **7**(2018).
32. Vogel, H*., et al.* GLP-1 and estrogen conjugate acts in the supramammillary nucleus to reduce food-reward and body weight. *Neuropharmacology* **110**, 396-406 (2016).
33. Shin, R. & Ikemoto, S. Administration of the GABA(A) receptor antagonist picrotoxin into rat supramammillary nucleus induces c-Fos in reward-related brain structures. Supramammillary picrotoxin and c-Fos expression. *BMC neuroscience* **11**(2010).
34. Ikemoto, S., Witkin, B.M., Zangen, A. & Wise, R.A. Rewarding effects of AMPA administration into the supramammillary or posterior hypothalamic nuclei but not the ventral tegmental area. *Journal of Neuroscience* **24**, 5758-5765 (2004).
35. Golden, S.A*., et al.* Basal forebrain projections to the lateral habenula modulate aggression reward. *Nature* **534**, 688-692 (2016).
36. Schino, G., D'Amato, F.R. & Troisi, A. Maternal aggression in lactating female Japanese macaques: time course and interindividual variation. *Can J Zool* **82**, 1975-1979 (2004).
37. Bosch, O.J. Maternal aggression in rodents: brain oxytocin and vasopressin mediate pup defence. *Philosophical Transactions of the Royal Society B-Biological Sciences* **368**(2013).
38. Maestripieri, D. & Alleva, E. Maternal Aggression and Litter Size in the Female House Mouse. *Ethology* **84**, 27-34 (1990).
39. Flannelly, K.J. & Kemble, E.D. The Effect of Pup Presence and Intruder Behavior on Maternal Aggression in Rats. *B Psychonomic Soc* **25**, 133-135 (1987).
40. Haney, M., Debold, J.F. & Miczek, K.A. Maternal Aggression in Mice and Rats Towards Male and Female Conspecifics. *Aggressive Behav* **15**, 443-453 (1989).
41. Mos, J., Olivier, B. & Vanoorschot, R. Maternal Aggression Towards Different Sized Male Opponents - Effect of Chlordiazepoxide Treatment of the Mothers and D-Amphetamine Treatment of the Intruders. *Pharmacol Biochem Be* **26**, 577-584 (1987).
42. Stagkourakis, S., Spigolon, G., Liu, G. & Anderson, D.J. Experience-dependent plasticity in an innate social behavior is mediated by hypothalamic LTP. *Proceedings of the National Academy of Sciences of the United States of America* **117**, 25789-25799 (2020).
43. Gandelman, R. Mice - Postpartum Aggression Elicited by Presence of an Intruder. *Hormones and behavior* **3**, 23-+ (1972).
44. Howard, S.M., Gandelman, R. & Rosenthal, C. Isolation Potentiates the Aggression-Activating Property of Testosterone in Female Mice. *Physiology & behavior* **26**, 971-972 (1981).
45. Barkley, M.S. & Goldman, B.D. Testosterone-Induced Aggression in Adult Female Mice. *Hormones and behavior* **9**, 76-84 (1977).

46. Erskine, M.S., Denenberg, V.H. & Goldman, B.D. Aggression in the lactating rat: effects of intruder age and test arena. *Behavioral biology* **23**, 52-66 (1978).
47. Flannelly, K.J. & Flannelly, L. Opponents' size influences maternal aggression. *Psychological reports* **57**, 883-886 (1985).
48. Hallak, M.D.M. & Hotra, J.W. Maternal serum hormone concentrations in Long-Evans rats. *J Trace Microprobe T* **21**, 103-110 (2003).
49. Dwyer, C.M. & Lawrence, A.B. Induction of maternal behaviour in non-pregnant, hormone-primed ewes. *Anim Sci* **65**, 403-408 (1997).
50. Duenhoelter, J.H. Maternal Hormone Measurements. *Jama-J Am Med Assoc* **248**, 1109-1109 (1982).
51. Hansult, C.D. & Kessler, S. Role of Hormones in Maternal Aggression and Infant Care. *Behavior genetics* **7**, 65-66 (1977).
52. Zarrow, M.X., Denenberg, V.H. & Gandelman, R. Prolactin - Is It an Essential Hormone for Maternal Behavior in Mammal. *Hormones and behavior* **2**, 343-+ (1971).
53. Riddle, O. Prolactin in Vertebrate Function and Organization. *Jnci-J Natl Cancer I* **31**, 1039-+ (1963).
54. Lhermite, M. Gonadotropin and Prolactin Function during Pregnancy and Postpartum. *Rev Fr Gynecol Obste* **71**, 159-165 (1976).
55. Moltz, H., Levin, R. & Leon, M. Prolactin in Postpartum Rat - Synthesis and Release in Absence of Suckling Stimulation. *Science* **163**, 1084-& (1969).
56. Riesen, J.W., Saiduddi.S, Graves, W.E., Tyler, W.J. & Casida, L.E. Pituitary Prolactin Activity in Postpartum Dairy Cows. *Journal of animal science* **25**, 929-& (1966).
57. Numan, M., Moltz, H. & Leon, M. Interference with Prolactin Release and Maternal Behavior of Female Rats. *Hormones and behavior* **3**, 29-& (1972).
58. Bridges, R.S., Goldman, B.D. & Bryant, L.P. Serum Prolactin Concentrations and Initiation of Maternal-Behavior in Rat. *Hormones and behavior* **5**, 219-226 (1974).
59. Brown, R.S.E.*, et al.* Prolactin action in the medial preoptic area is necessary for postpartum maternal nursing behavior. *Proceedings of the National Academy of Sciences of the United States of America* **114**, 10779-10784 (2017).
60. Pedersen, C.A. & Prange, A.J., Jr. Induction of maternal behavior in virgin rats after intracerebroventricular administration of oxytocin. *Proceedings of the National Academy of Sciences of the United States of America* **76**, 6661-6665 (1979).
61. Pedersen, C.A., Ascher, J.A., Monroe, Y.L. & Prange, A.J., Jr. Oxytocin induces maternal behavior in virgin female rats. *Science* **216**, 648-650 (1982).
62. Watarai, A.*, et al.* The blockade of oxytocin receptors in the paraventricular thalamus reduces maternal crouching behavior over pups in lactating mice. *Neuroscience letters* **720**, 134761 (2020).
63. Champagne, F., Diorio, J., Sharma, S. & Meaney, M.J. Naturally occurring variations in maternal behavior in the rat are associated with differences in estrogen-inducible central oxytocin receptors. *Proceedings of the National Academy of Sciences of the United States of America* **98**, 12736-12741 (2001).
64. Guillou, A.*, et al.* Assessment of lactotroph axis functionality in mice: longitudinal monitoring of PRL secretion by ultrasensitive-ELISA. *Endocrinology* **156**, 1924-1930 (2015).
65. Gouilleux, F., Wakao, H., Mundt, M. & Groner, B. Prolactin Induces Phosphorylation of Tyr694 of Stat5 (Mgf), a Prerequisite for DNA-Binding and Induction of Transcription. *Embo Journal* **13**, 4361-4369 (1994).
66. DaSilva, L.*, et al.* Prolactin recruits STAT1, STAT3 and STAT5 independent of conserved receptor tyrosines TYR402, TYR479, TYR515 and TYR580. *Molecular and cellular endocrinology* **117**, 131-140 (1996).
67. Ali, S. & Ali, S. Prolactin receptor regulates Stat5 tyrosine phosphorylation and nuclear translocation by two separate pathways. *Journal of Biological Chemistry* **273**, 7709-7716 (1998).
68. Lerant, A., Kanyicska, B. & Freeman, M.E. Nuclear translocation of STAT5 and increased expression of Fos related antigens (FRAs) in hypothalamic dopaminergic neurons after prolactin administration. *Brain research* **904**, 259-269 (2001).

69. Brockman, J.L. & Schuler, L.A. Prolactin signals via Stat5 and Oct-1 to the proximal cyclin D1 promoter. *Molecular and cellular endocrinology* **239**, 45-53 (2005).
70. Cave, B.J.*, et al.* Prolactin-induced activation of STAT5 within the hypothalamic arcuate nucleus. *Neuroreport* **16**, 1423-1426 (2005).
71. Jaroenporn, S., Nagaoka, K., Ohta, R., Watanabe, G. & Taya, K. Prolactin induces phosphorylation of the STAT5 in adrenal glands of Hatano rats during stress. *Life sciences* **85**, 172-177 (2009).
72. Buntin, J.D. & Buntin, L. Increased STAT5 signaling in the ring dove brain in response to prolactin administration and spontaneous elevations in prolactin during the breeding cycle. *General and comparative endocrinology* **200**, 1-9 (2014).
73. Brown, R.S.E., Kokay, I.C., Herbison, A.E. & Grattan, D.R. Distribution of Prolactin-Responsive Neurons in the Mouse Forebrain. *Journal of Comparative Neurology* **518**, 92-102 (2010).
74. Augustine, R.A.*, et al.* Prolactin regulation of oxytocin neurone activity in pregnancy and lactation. *J Physiol-London* **595**, 3591-3605 (2017).
75. Brown, R.S.E., Herbison, A.E. & Grattan, D.R. Effects of Prolactin and Lactation on A15 Dopamine Neurones in the Rostral Preoptic Area of Female Mice. *Journal of neuroendocrinology* **27**, 708-717 (2015).
76. Brown, R.S.E., Piet, R., Herbison, A.E. & Grattan, D.R. Differential Actions of Prolactin on Electrical Activity and Intracellular Signal Transduction in Hypothalamic Neurons. *Endocrinology* **153**, 2375-2384 (2012).
77. Silveira, M.A.*, et al.* Acute effects of somatomammotropin hormones on neuronal components of the hypothalamic-pituitary-gonadal axis. *Brain research* **1714**, 210-217 (2019).
78. Sabatini, B.L. & Regehr, W.G. Control of neurotransmitter release by presynaptic waveform at the granule cell to Purkinje cell synapse. *The Journal of neuroscience : the official journal of the Society for Neuroscience* **17**, 3425-3435 (1997).
79. Kamikawa, A. & Seko, J. Physiological and pharmacological evaluation of oxytocin-induced milk ejection in mice. *Experimental animals* **69**, 345-353 (2020).
80. Wang, Y.F. & Hatton, G.I. Milk ejection burst-like electrical activity evoked in supraoptic oxytocin neurons in slices from lactating rats. *Journal of neurophysiology* **91**, 2312-2321 (2004).
81. Donker, J.D., Koshi, J.H. & Petersen, W.E. The effect of exogenous oxytocin in blocking the normal relationship between endogenous oxytocic substance and the milk ejection phenomenon. *Science* **119**, 67-68 (1954).
82. Finkenwirth, C., Martins, E., Deschner, T. & Burkart, J.M. Oxytocin is associated with infant-care behavior and motivation in cooperatively breeding marmoset monkeys. *Hormones and behavior* **80**, 10-18 (2016).
83. Ross, H.E. & Young, L.J. Oxytocin and the neural mechanisms regulating social cognition and affiliative behavior. *Frontiers in neuroendocrinology* **30**, 534-547 (2009).
84. Stohn, J.P.*, et al.* Increased aggression and lack of maternal behavior in Dio3-deficient mice are associated with abnormalities in oxytocin and vasopressin systems. *Genes Brain and Behavior* **17**, 23-35 (2018).
85. Bosch, O.J., Meddle, S.L., Beiderbeck, D.I., Douglas, A.J. & Neumann, I.D. Brain oxytocin correlates with maternal aggression: Link to anxiety. *Journal of Neuroscience* **25**, 6807-6815 (2005).
86. Kremarik, P., Freund-Mercier, M.J. & Stoeckel, M.E. Oxytocin and vasopressin binding sites in the hypothalamus of the rat: histoautoradiographic detection. *Brain research bulletin* **36**, 195-203 (1995).
87. Zaninetti, M. & Raggenbass, M. Oxytocin receptor agonists enhance inhibitory synaptic transmission in the rat hippocampus by activating interneurons in stratum pyramidale. *The European journal of neuroscience* **12**, 3975-3984 (2000).
88. Elands, J., Barberis, C. & Jard, S. [3H]-[Thr4,Gly7]OT: a highly selective ligand for central and peripheral OT receptors. *The American journal of physiology* **254**, E31-38 (1988).
89. Gruskos, J., Goldwaser, A. & Guarracino, D.A. Competition of peptide hormone mimics with vasopressin and oxytocin for binding their target membrane receptors. *Abstr Pap Am Chem S* **244**(2012).

524 90. Hibert, M.*, et al.* Functional architecture of vasopressin/oxytocin receptors. *Journal of receptor and*
525 *signal transduction research* **19**, 589-596 (1999).
526 91. Zingg, H.H. Vasopressin and oxytocin receptors. *Bailliere Clin Endoc* **10**, 75-96 (1996).
527 92. Manning, M., Stoev, S., Chan, W.Y. & Sawyer, W.H. Receptor-Specific Antagonists of Vasopressin and
528 Oxytocin - a Current Perspective. *Neurohypophysis : A Window on Brain Function* **689**, 219-232 (1993).
529 93. Jard, S., Elands, J., Schmidt, A. & Barberis, C. Vasopressin and Oxytocin Receptors - an Overview.
530 *Progress in Endocrinology 1988, Vol 1 and 2* **799**, 1183-1188 (1988).
531 94. Martin, P.J. & Schild, H.O. Interaction of Oxytocin and Vasopressin with Tissue Receptors. *Biochemical*
532 *pharmacology* **12**, 139-& (1963).
533 95. St John, R.D. & Corning, P.A. Maternal aggression in mice. *Behavioral biology* **9**, 635-639 (1973).
534 96. Zimprich, A.*, et al.* Assessing Sociability, Social Memory, and Pup Retrieval in Mice. *Current protocols*
535 *in mouse biology* **7**, 287-305 (2017).
536 97. Bendesky, A.*, et al.* The genetic basis of parental care evolution in monogamous mice. *Nature* **544**,
537 434-439 (2017).
538 98. Moyer, K.E. Kinds of aggression and their physiological basis. *Communications in Behavioral Biology*,
539 p. 65-87. (1968).
540 99. Yang, C.F.*, et al.* Sexually dimorphic neurons in the ventromedial hypothalamus govern mating in both
541 sexes and aggression in males. *Cell* **153**, 896-909 (2013).
542 100. Lee, H.*, et al.* Scalable control of mounting and attack by Esr1+ neurons in the ventromedial
543 hypothalamus. *Nature* **509**, 627-632 (2014).
544 101. Unger, E.K.*, et al.* Medial Amygdalar Aromatase Neurons Regulate Aggression in Both Sexes. *Cell*
545 *Reports* **10**, 453-462 (2015).
546 102. Falkner, A.L., Grosenick, L., Davidson, T.J., Deisseroth, K. & Lin, D. Hypothalamic control of male
547 aggression-seeking behavior. *Nat Neurosci* **19**, 596-604 (2016).
548 103. Liu, M., Kim, D.W., Zeng, H. & Anderson, D.J. Make war not love: The neural substrate underlying a
549 state-dependent switch in female social behavior. *Neuron* **110**, 841-856 e846 (2022).
550 104. Beach, F.A. Hormonal Modification of Sexually Dimorphic Behavior. *Psychoneuroendocrinology* **1**, 3-+
551 (1975).
552 105. Kimchi, T., Xu, J. & Dulac, C. A functional circuit underlying male sexual behaviour in the female mouse
553 brain. *Nature* **448**, 1009-1014 (2007).
554 106. Brunton, P.J., Russell, J.A. & Douglas, A.J. Adaptive responses of the maternal hypothalamic-pituitary-
555 adrenal axis during pregnancy and lactation. *Journal of neuroendocrinology* **20**, 764-776 (2008).
556 107. Pedersen, C.A. & Prange, A.J. Induction of Maternal-Behavior in Virgin Rats after
557 Intracerebroventricular Administration of Oxytocin. *Proceedings of the National Academy of Sciences*
558 *of the United States of America* **76**, 6661-6665 (1979).
559 108. Bridges, R.S., DiBiase, R., Loundes, D.D. & Doherty, P.C. Prolactin stimulation of maternal behavior in
560 female rats. *Science* **227**, 782-784 (1985).
561 109. Wise, D.A. & Pryor, T.L. Effects of ergocornine and prolactin on aggression in the postpartum golden
562 hamster. *Hormones and behavior* **8**, 30-39 (1977).
563 110. Gleason, P.E., Michael, S.D. & Christian, J.J. Brief report prolactin-induced aggression in female
564 Peromyscus leucopus. *Behavioral and neural biology* **33**, 243-248 (1981).
565 111. Ferris, C.F.*, et al.* Oxytocin in the Amygdala Facilitates Maternal Aggression. *Annals of the New York*
566 *Academy of Sciences* **652**, 456-457 (1992).
567 112. DeVries, A.C., Young, W.S. & Nelson, R.J. Reduced aggressive behaviour in mice with targeted
568 disruption of the oxytocin gene. *Journal of neuroendocrinology* **9**, 363-368 (1997).
569 113. Bosch, O.J. & Neumann, I.D. Both oxytocin and vasopressin are mediators of maternal care and
570 aggression in rodents: from central release to sites of action. *Horm Behav* **61**, 293-303 (2012).
571 114. Erskine, M.S., Barfield, R.J. & Goldman, B.D. Postpartum aggression in rats: II. Dependence on
572 maternal sensitivity to young and effects of experience with pregnancy and parturition. *J Comp Physiol*
573 *Psychol* **94**, 495-505 (1980).

574 115. Georgescu, T., Khant Aung, Z., Grattan, D.R. & Brown, R.S.E. Prolactin-mediated restraint of maternal
575 aggression in lactation. *Proceedings of the National Academy of Sciences of the United States of*
576 *America* **119**(2022).
577 116. Lin, D.*, et al.* Functional identification of an aggression locus in the mouse hypothalamus. *Nature* **470**,
578 221-226 (2011).
579 117. Kohl, J.*, et al.* Functional circuit architecture underlying parental behaviour. *Nature* **556**, 326-331
580 (2018).
581 118. Ekstrand, M.I.*, et al.* Progressive parkinsonism in mice with respiratory-chain-deficient dopamine
582 neurons. *Proceedings of the National Academy of Sciences of the United States of America* **104**, 1325-
583 1330 (2007).
584 119. Franklin, K.B.J. & Paxinos, G. *THE MOUSE BRAIN IN STEREOTACTIC COORDINATES*, (2008).
585 120. Behringer, R., Gertsenstein, M., Nagy, K.V. & Nagy, A. Selecting Female Mice in Estrus and Checking
586 Plugs. *Cold Spring Harb Protoc* **2016**(2016).

587 ## Materials and methods

588 **Animals.** All animal experiments had received approval from the local ethical board, *Stockholms*
589 *Norra Djurförsöksetiska Nämnd*, and were performed in accordance with the European Communities
590 Council Directive of November 24, 1986 (86/609/EEC). Wild-type mice with C57BL/6J and BALB/c
591 background were used, in addition to previously generated C57BL/6J *Slc6a*^{Cre} (DAT-Cre) knock-in[118]
592 and floxed-tdTomato mice (The Jackson Laboratory, strain datasheet – 007909). Animals were group-
593 housed, up to five per cage, in a temperature (23°C) and humidity (55%) controlled environment, in a
594 12h light, 12h dark cycle with *ad libitum* access to food and water. Cages were changed on a weekly
595 basis.

596 Adult virgin female, and lactating female mice used in experiments were single housed for a period
597 of two to four weeks, depending on the experimental design. Only multiparous lactating mice were
598 used in the experimental group of *lactating dams*, typically following their third or fourth parturition.

599

600 **Viral vectors.** For channelrhodopsin optogenetic studies animals were injected in the PMv with
601 400 nL of AAV5-EF1a-DIO-hChR2(H134R)-eYFP-WPRE-hGH (Addgene20298) 8.41 × 10^{12} genomic
602 copies per mL. For halorhodopsin-mediated neuronal silencing, animals were injected with 400 nL of
603 AAV5-EF1a-DIO-eNpHR3.0-eYFP-WPRE-hGH (Addgene26966) 7.02 × 10^{12} genomic copies per mL.
604 The control groups in optogenetic were injected with 400 nL of AAV5-EF1a-DIO-eYFP-WPRE-hGH
605 (Addgene27056) 5.82 × 10^{12} genomic copies per mL. The ChR2, eNpHR3 and eYFP AAV5 were
606 prepared by the University of Pennsylvania Vector Core. For targeted cell ablation of PMv^{DAT} neurons
607 animals were injected in PMv with 300 nL of AAV5-flex-taCasp3-TEVp 2.9 × 10^{12} genomic copies per
608 mL, and the AAV was prepared by the viral vector core at the University of North Carolina. Viral
609 injections were performed bilaterally.

610

611 **Stereotactic surgery and viral gene transfer.** Adult DAT-Cre mice 5-8 months old (sexually
612 inexperienced) were stereotactically injected with a virus, and implanted with fiber implants when
613 purposed for *in vivo* optogenetic behaviour experiments, and were individually housed for 2 weeks
614 post-surgery. Animals were anaesthetised with isoflurane (1–5%) and placed in a stereotactic frame
615 (David Kopf Instruments). Virus was injected into the PMv bilaterally using a pulled glass capillary
616 (World Precision Instruments) by nanolitre pressure injection at a flow rate of 50 nL per min (Micro4
617 controller, World Precision Instruments; Nanojector II, Drummond Scientific). Stereotactic injection
618 coordinates to target the PMv were obtained from the Paxinos and Franklin atlas[119] (Bregma: -2.45
619 mm, midline ±0.6 mm, dorsal surface -5.5 mm). Ferrules and fiber-optic patch cords were purchased
620 from Thorlabs and Doric Lenses, respectively. The virus-injected animals were housed individually
621 during a 2-week recovery period, and then examined behaviourally and histologically.

622 In the case of the *lactating dams* group, sexually experienced female mice with prior maternal
623 experience were placed in a cage with a male mouse, and were checked for plugs in the morning
624 hours of the next four days[120]. Following identification of plugs, female mice were single housed, and
625 surgeries were performed for AAV injections, and/or optic fiber implants, as above. The surgical
626 procedures occurred within a week of plug identification. Female mice in which plug identification did
627 not occur or was ambiguous were excluded from the study.
628
629 **Optogenetics.** In optogenetic experiments, subjects were coupled via a ferrule patch cord to a
630 ferrule on the head of the mouse using a zirconia split sleeve (Doric Lenses). The optical fiber was
631 connected to a laser (447 nm for ChR2; 635 nm for eNpHR3; CNI-MLL-III-447-200-5-LED and CNI-
632 MLL-III-635-200-5-LED, CNI lasers 200 mW) via a fiber-optic rotary joint (FRJ_1x1_FC-FC, Doric
633 Lenses) to avoid twisting of the cable caused by the animal's movement. After a testing session, DAT-
634 Cre animals were uncoupled from the fiber-optic cable and returned to a housing room. The frequency
635 and duration of photostimulation were controlled using custom written LabView software. Laser power
636 was controlled by dialling an analogue knob on the power supply of the laser sources. Light power
637 was measured from the tip of the ferrule in the patch cord before being installed in the brain (the
638 ferrule-connector system) at different laser output settings, using an optical power and energy meter
639 and a photodiode power sensor (Thorlabs). Upon identification of the fiber placement coordinates in
640 brain tissue slides, irradiance (light intensity) was calculated using the brain tissue light transmission
641 calculator based on (http://www.stanford.edu/group/dlab/cgi-bin/graph/chart.php) using laser power
642 measured at the tip and the distance from the tip to the target brain region measured by histology.
643 Animals showing no detectable viral expression in the target region and/or ectopic fiber placement
644 were excluded from analysis. In some experiments, animals were photostimulated with a train of 473
645 nm light (20 Hz, 5 msec, 5 min) 45 min before perfusion in the absence of an intruder at an intensity
646 which had evoked a behavioural phenotype in the final testing session. Brain sections were
647 subsequently immunohistochemically labelled for c-Fos to identify optogenetically activated cells.
648
649 **Behavioural tests.** Behavioural tests were performed at 2h post-initiation of the light phase and
650 2h prior to initiation of the dark phase. Mice were acclimated to the testing facility for 1 h prior to
651 testing. Behaviours were recorded using a digital video recording unit. Behavioural annotations were
652 performed manually, with conditions blinded to the experimenter performing the behavioural scoring.
653
654 **Resident-intruder (RI) test.** RI tests were initiated at 2 to 4 weeks post-surgery and repeated
655 weekly for 2 to 5 weeks. All dams used in the present study were multiparous and were used in
656 behavioural experiments during their third or fourth litter. Mouse cages were not cleaned for a
657 minimum of 3 days prior to the behavioural test. Intruders were individually introduced to a DAT-Cre
658 mouse in a testing session in a random order with respect to sex, with a 5 min interval between

intruders. The types of intruders were: juvenile females and adult females. Subjects involved in the RI test were exposed to 3 experimental days of the test, resulting in multiple measurements per resident.

ChR2-mediated activation in RI. After the introduction of an intruder, a virus-injected animal was recorded for 3 min to assess baseline behaviour towards each intruder. The baseline recording was followed by photostimulation trials (3 min in duration) with varying irradiance (intensity), stimulation intervals, distance, orientation and recent behaviour history between the two animals at the onset of photostimulation. The AAV5-DIO-eYFP and AAV5-DIO-ChR2 injected experimental animals were processed in random order.

eNpHR3-mediated silencing in RI. DAT-Cre lactating females expressing eNpHR3 or control eYFP were introduced to between one to four juvenile female intruders, in three acclimation sessions without photostimulation to assess baseline aggression as well as to augment aggressiveness. Testing sessions initiated with recordings in the absence of laser stimulation to assess baseline behaviour towards each intruder on the day of the experiment. In photostimulation trials, irradiance (intensity) ranging from 2.1 – 11.6 mW/mm^2 was delivered continuously in varying intervals (typically 2-10 sec) depending on the phase of the resident-intruder interaction. To examine whether photostimulation during charging stopped escalation to attack, residents were photostimulated during body realignment to gain access to the back of the intruder.

Pup retrieval test. Adult virgin female or lactating mice 5-8 months old were exposed to foster pups or to their own litter, respectively. The litter size per test is described in the individual tests/figures. Material for nest building was provided in each cage. The activity in the cage was video recorded, and maternal behaviours were scored by an experimenter blinded to the experimental conditions.

Three-chambered sociability test. The social approach apparatus was an open-topped box made of acrylic (60 cm in length × 40 cm in width × 20 cm in height), and divided into three chambers with two clear acrylic walls. Dividing walls had retractable doorways allowing access into each chamber. The wire cup used to contain the novel mice was made of cylindrical chrome bars spaced 1 cm apart (10 cm H; bottom diameter: 10 cm). Test mice were confined in the center chamber at the beginning of each phase. Exploration of an enclosed mouse or an empty wire cup was defined as when a test mouse oriented toward the cup with the distance between the nose and the cup less than 1 cm, or as climbing on the cup. The time spent in each chamber and time spent exploring enclosed novel mice or empty cups (the novel objects) were recorded from an overhead camera, and analyzed using Ethovision XT12.

696

697 **Open field test (OFT).** OFTs were performed in a white acrylic glass box (45 × 45 × 40 cm) with
698 an overhead lamp directed to the centre of the field, providing 120 lux of illumination on the floor of
699 the arena. Each mouse was placed in the corner of the apparatus and locomotion parameters were
700 recorded for 20 min.

701

702 **Elevated plus maze (EPM).** The EPM test was performed using a polyvinyl chloride maze
703 comprising a central part (5x5 cm), two opposing open arms (32.5x5 cm), and two opposing closed
704 arms (32.5x5x32.5 cm). The apparatus was set to a height of 50 cm, and the open arms were provided
705 with uniform overhead illumination of 6 lux. Mice were placed in the open arm point close to the centre
706 facing the closed arms, and video recordings were performed for a total duration of 20 min.

707

708 **Chronic administration of maternal hormones in the PMv.** For localised chronic administration
709 of maternal hormones in the PMv, we performed cannula implantations using the Paxinos and
710 Franklin atlas[119] coordinates (Bregma: -2.45 mm, midline ±0.6 mm, dorsal surface -5.5 mm). Cannulae
711 (0008663 Brain Infusion Kit 2) and osmotic minipumps (0000298 ALZET Model 2004) were
712 purchased from ALZET, and prepared according to protocol.

713

714 **Brain slice electrophysiology.** Acute slices of the mediobasal hypothalamus were prepared
715 from adult DAT-tdTomato mice (own breeding). Slices were cut on a vibratome (Leica VT1000S) to
716 250 µm thickness and continuously perfused with oxygenated aCSF containing (in millimolar): NaCl
717 (127), KCl (2.0), NaH_2PO_4 (1.2), $NaHCO_3$ (26), $MgCl_2$ (1.3), $CaCl_2$ (2.4), and D-glucose (10), at near-
718 physiological temperature (33±1°C) during recording. Each slice was exposed only to a single bath
719 application of pharmacological compounds and was used for a single experiment. Whole-cell current-
720 and voltage-clamp recordings were performed with micropipettes filled with intracellular solution
721 containing (in millimolar), K-gluconate (140), KCl (10), HEPES (10), EGTA (10), and Na_2ATP (2) (pH
722 7.3 with KOH). Recordings were performed using a Multiclamp 700B amplifier, a DigiData 1440
723 digitiser, and pClamp 10.2 software (Molecular Devices). Slow and fast capacitative components were
724 semi-automatically compensated. Access resistance was monitored throughout the experiments, and
725 neurons in which the series resistance exceeded 15 MΩ or changed ≥20% were excluded from the
726 statistics. Liquid junction potential was 16.4 mV and not compensated. The recorded current was
727 sampled at 20 kHz.

728 Reagents used in slice electrophysiology experiments; Neurobiotin™ tracer (Vector laboratories)
729 was used in combination with Streptavidin, DyLight™ 405 conjugated (21831 Thermoscientific) or
730 Avidin-FITC (43-4411 Invitrogen). TTX was purchased from Alomone Labs. Oxytocin nonapeptide,
731 the OT-receptor (OT-R) agonist, (Thr4, Gly7)-oxytocin (TGOT), and the OT-R antagonist, vasotocin
732 [$d(CH2)_5^1$, $Tyr(Me)^2$, Thr^4, Orn^8, des-Gly NH_2^9], were purchased from Bachem. Prolactin CYT-321 was

purchased from PROSPEC, and SR 95531 (Gabazine) and ML-218 hydrochloride were purchased from Tocris. Matlab and OriginPro8 were used for electrophysiological data analysis.

Immunofluorescence. Mice were anaesthetised with sodium pentobarbital (200 mg/kg, i.p., Sanofi-Aventis), then transcardially perfused with 10 mL Ca^{2+}-free Tyrode's solution (37°C) containing 0.2% heparin, followed by 10 mL fixative (4% paraformaldehyde and 0.4% picric acid in 0.16 M phosphate buffer (PBS), 37°C), then 50 mL ice cold fixative. Whole brains were dissected, immersed in ice cold fixative for 90 min then stored in 0.1M PBS (pH 7.4) containing 20% sucrose, 0.02% bacitracin and 0.01% sodium azide for three days, before freezing with CO_2. Coronal sections were cut at a thickness of 14 µm on a cryostat (Microm) and thaw-mounted onto gelatin-coated glass slides. For indirect immunofluorescence staining (performed at room temperature unless otherwise specified), air-dried sections were washed in 0.01 M PBS for 30 min before incubation with primary antisera diluted in PBS containing 0.3% Triton X-100 and 1% BSA for 16 hours at 4°C. The slides were then washed for 30 min in PBS followed by 2h incubation with Alexa-488-conjugated donkey anti-rabbit secondary antisera (1:500; Invitrogen). Slides went through a final wash for 30 min in PBS and mounted with glycerol containing (2.5% DABCO; Sigma). This method was used with the following antibodies: NeuN was detected with primary antibody rabbit anti-NeuN (1:500; Cell Signalling, D4G40), eYFP was detected with chicken anti-GFP (1:500; Aves Labs, GFP-1020). Immunohistochemistry for pSTAT5: Prior to immunofluorescence staining, antigen retrieval was performed by incubating sections for 15 min in citric acid (pH 7.4) at 80°C, then cooled at room temperature for a further 30 min. After a 1% H_2O_2 Tris-buffered wash, sections were incubated in rabbit pSTAT5 primary antibody (pSTAT5 Tyr 694, Cat#: C11C5, 1:500; Cell Signaling Technology) for 72 hours at 4°C. Primary antibody incubation was followed by Alexa-488-conjugated donkey anti-rabbit secondary antisera (1:500; Invitrogen).

To perform c-fos immunostaining, mice were deeply anesthetised with sodium pentobarbital (as described above) and perfused transcardially with 4% (weight/vol) ice-cold paraformaldehyde in 0.1M PBS. Brains were post-fixed in the same solution and 40 µm-thick coronal slices were cut at the vibratome (Leica). Two PMv coronal sections per animal were selected to perform c-fos immunostaining as follows. Sections were washed in TBS (100 mM Tris-Cl, 150 mM NaCl, pH 7.5), incubated 1h at 25ºC in 1% BSA-0.3% Triton X-100-TBS solution and then kept at 4°C in rabbit anti-c-fos antibody (sc-52 LotG1108, Santa Cruz Biotechnology) solution (1:200 in 1% BSA-TBS) overnight. After TBS washing, sections were incubated for 1h at 25ºC in Alexa Fluor® 647 (Invitrogen) goat anti-rabbit secondary antibody (1:500 in 1% BSA-TBS).

Microscopy and cell-counting. All brain slices were imaged by epifluorescence microscopy (ZEISS Imager M1) or confocal microscopy (Zeiss, LSM 800) for subsequent analysis. Brain areas were determined according to their anatomy using Paxinos and Franklin Brain Atlas[119]. For PMv^{DAT}

770 cell counts the entire PMv was cut, stained and counted. Quantification of c-fos staining was obtained
771 by averaging the number of positive cells of right and left PMv in two brain sections (-2.46 and -2.54
772 mm from Bregma[119]). All counts were performed manually using Image J software and blind to test
773 conditions.
774
775 **Randomization and blinding.** Behavioural data collection and analysis was performed blind to
776 experimental conditions. Anatomy data analysis but not tissue collection was blinded.
777 Electrophysiological data sampling and analysis was not blinded, with the exception of all whole-cell
778 patch clamp datasets presented in Figure 1. Mice were first screened for expressing maternal
779 aggression and then further assigned to groups for behavioural experiments.
780
781 **Statistical analysis.** No statistical methods were used to pre-determine sample sizes but our
782 sample sizes are similar to those reported in previous publications[2,11,14,30,31]. Data met the
783 assumptions of the statistical tests used, and were tested for normality and equal variance. All *t*-tests
784 and one-way ANOVAs were performed using Graph Pad Prism software (Graphpad Software Inc.).
785 The Tukey and Bonferroni *posthoc* tests were used as appropriate for one-way ANOVAs. Normality
786 was determined by D'Agostino–Pearson normality test. Statistical significance was set at $P < 0.05$.
787
788 **Data availability statement.** The data that support the findings of this study are available from
789 the corresponding authors upon request.

Figures

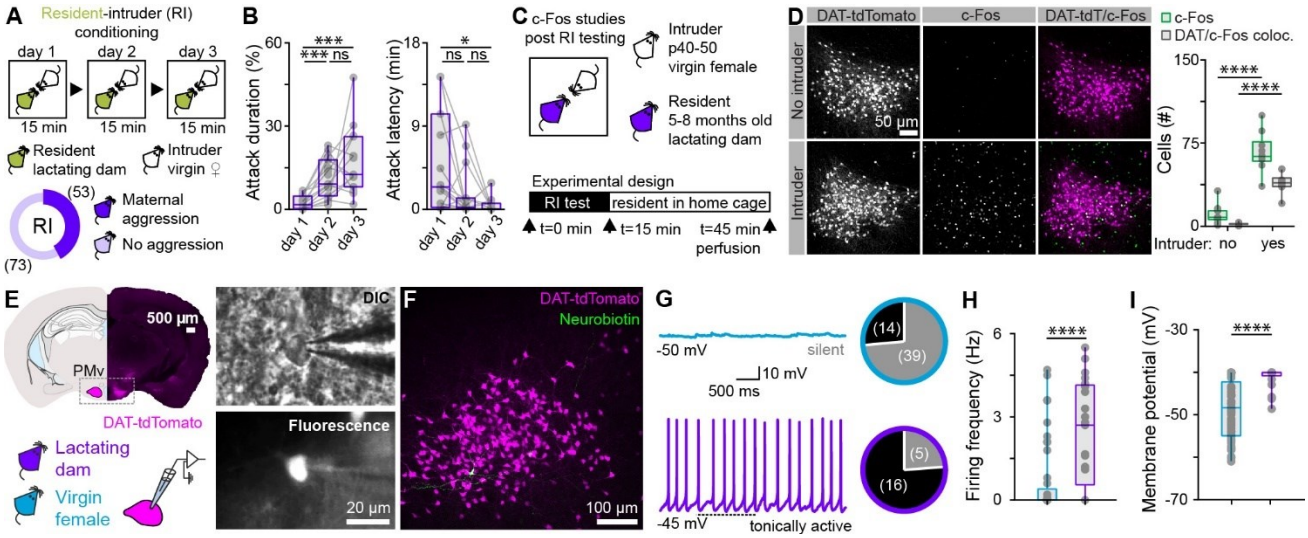

Figure 1. PMv^{DAT} neurons activate in lactating dams following an aggressive encounter and are electrically hyperexcitable during the nursing state.

(A) Schematic representation of the experimental design used to identify lactating dams expressing maternal aggression (n = 126 lactating mice). Lactating dams were between five and eight months of age.

(B) Quantification of maternal aggression traits identify increased attack duration (left; shown as the percentage of total session time) and decreased attack latency (right) with consecutive trials in the resident-intruder (RI) paradigm shown in Figure 1A (n = 15 mice per group, RM one-way ANOVA, p = 0.0010).

(C) Schematic representation of the experimental design used to perform c-Fos studies following RI testing.

(D) Confocal images of c-Fos immunoreactivity in the PMv post-RI testing in the absence (top panels) or presence (bottom panels) of a juvenile female conspecific (n = 12 sections from 6 mice without intruder exposure, and n = 10 sections from 5 mice with intruder exposure; comparisons performed using two-tailed unpaired *t*-test, p < 0.0001).

(E) Identification of PMv^{DAT} neurons using the DAT-tdTomato mouse line to perform whole-cell patch clamp slice recordings from age-matched adult virgin female and lactating mice (five to eight months old).

(F) PMv^{DAT} neurons were identified and reconstructed following the recording session using Neurobiotin-FITC.

(G) Example recordings from PMv^{DAT} neurons (left) and group data in pie charts (right) from virgin female (blue) and lactating (purple) mice, exhibiting low (gray) *vs* high (black) baseline spike discharge, respectively (n = 53 and 21 recorded cells from 26 virgin female and 11 lactating dams, respectively).

824 (H) Quantification of firing frequency in PMv^{DAT} cells in virgin females *vs* lactating dams (n = 53 vs 21
825 cells, two-tailed unpaired t-test, $p < 0.0001$).
826 (I) Quantification of membrane potential in PMv^{DAT} cells in virgin females *vs* lactating dams (n = 53 vs
827 21 cells, two-tailed unpaired t-test, $p < 0.0001$).
828 See also Table S1.

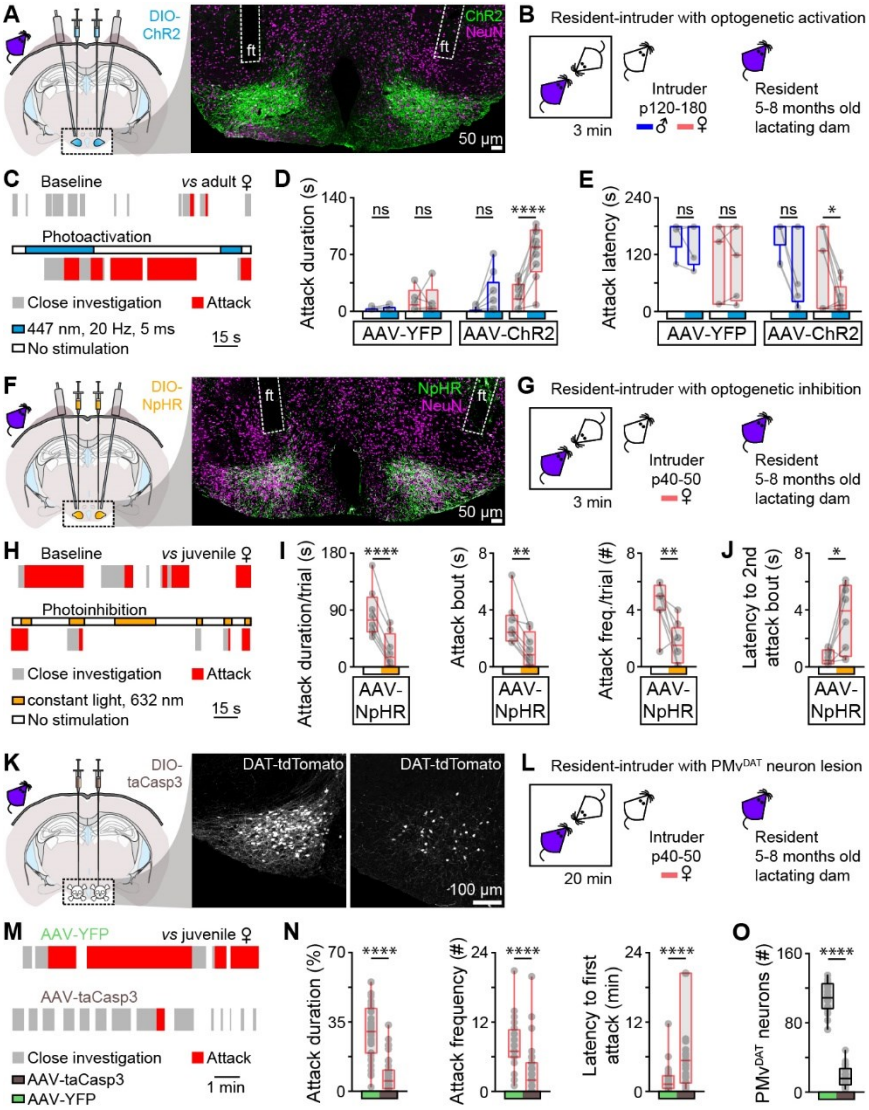

Figure 2. Manipulation of the PMv^{DAT} neuron activity allows bidirectional control of maternal aggression.

(A) Bilateral Cre-dependent ChR2 transduction and fiber implants in the PMv of lactating dams (left) and confocal image of a sample section counterstained with the pan-neuronal marker NeuN, used to validate ChR2 expression and stereotactic implantation coordinates (right).

(B) Schematic of the experimental design used to perform ChR2 PMv^{DAT} neuron photoactivation in the resident lactating dam during resident-intruder (RI) testing. Adult male and female intruders were used to minimise the levels of maternal aggression expressed in baseline conditions [40,47].

(C) Sample behaviour raster plots at baseline (top) and during ChR2 stimulation (bottom) in a lactating dam during a RI test.

(D) Attack duration with and without photostimulation in lactating dams injected with eYFP or ChR2, during the RI test against adult male or adult female intruders (n = 5-9 mice per group, ordinary one-way ANOVA, $p < 0.0001$).

860 (E) Attack latency with and without photostimulation in lactating dams injected with eYFP or ChR2,
861 during the RI test against adult male or adult female intruders (n = 5-9 mice per group, ordinary one-
862 way ANOVA, p = 0.0027).
863 (F) Bilateral Cre-dependent eNpHR3 transduction and fiber implants in the PMv of lactating dams
864 (left) and confocal image of a sample section counterstained with the pan-neuronal marker NeuN,
865 used to validate eNpHR3 expression and stereotactic implantation coordinates (right).
866 (G) Schematic of the experimental design used to perform eNpHR3 PMv^{DAT} neuron photoinhibition
867 studies in the resident lactating dam during RI testing.
868 (H) Sample behaviour raster plots during baseline and eNpHR3 mediated photoinhibition in a lactating
869 dam during a RI test.
870 (I) Quantification of aggression parameters (n = 8 mice per group, two-tailed paired t-test, p < 0.0001,
871 p = 0.0011, and p = 0.0071 respectively).
872 (J) Quantification of the latency to an attack bout following a photoinhibition episode (n = 8 mice per
873 group, two-tailed paired t-test, p = 0.0131).
874 (K) Bilateral Cre-dependent taCasp3 transduction in the PMv of lactating dams (left) and sample
875 confocal image sections following injection of eYFP (middle) *vs* taCasp3 (right), used to validate the
876 extent of the PMv^{DAT} cell lesion.
877 (L) Schematic of the experimental design used to perform RI tests in lactating dams with complete or
878 partial lesion of the PMv^{DAT} cells.
879 (M) Sample behaviour raster plots in control *vs* PMv^{DAT} neuron lesioned lactating dams during a RI
880 test.
881 (N) Quantification of aggression parameters (n = 34 trials per group, 12 mice per group, two-tailed
882 unpaired t-test, p < 0.0001, p < 0.0001, and p < 0.0001 respectively). All but two mice were tested
883 three times in the RI test. Two mice, one from each group, were tested twice in the RI test.
884 (O) Quantification of PMv^{DAT} neurons in eYFP and taCasp3 injected mice (n = 24 sections per group,
885 duplicates from 12 mice per group, two-tailed unpaired t-test, p < 0.0001).
886 See also Table S1, and Figure S1.

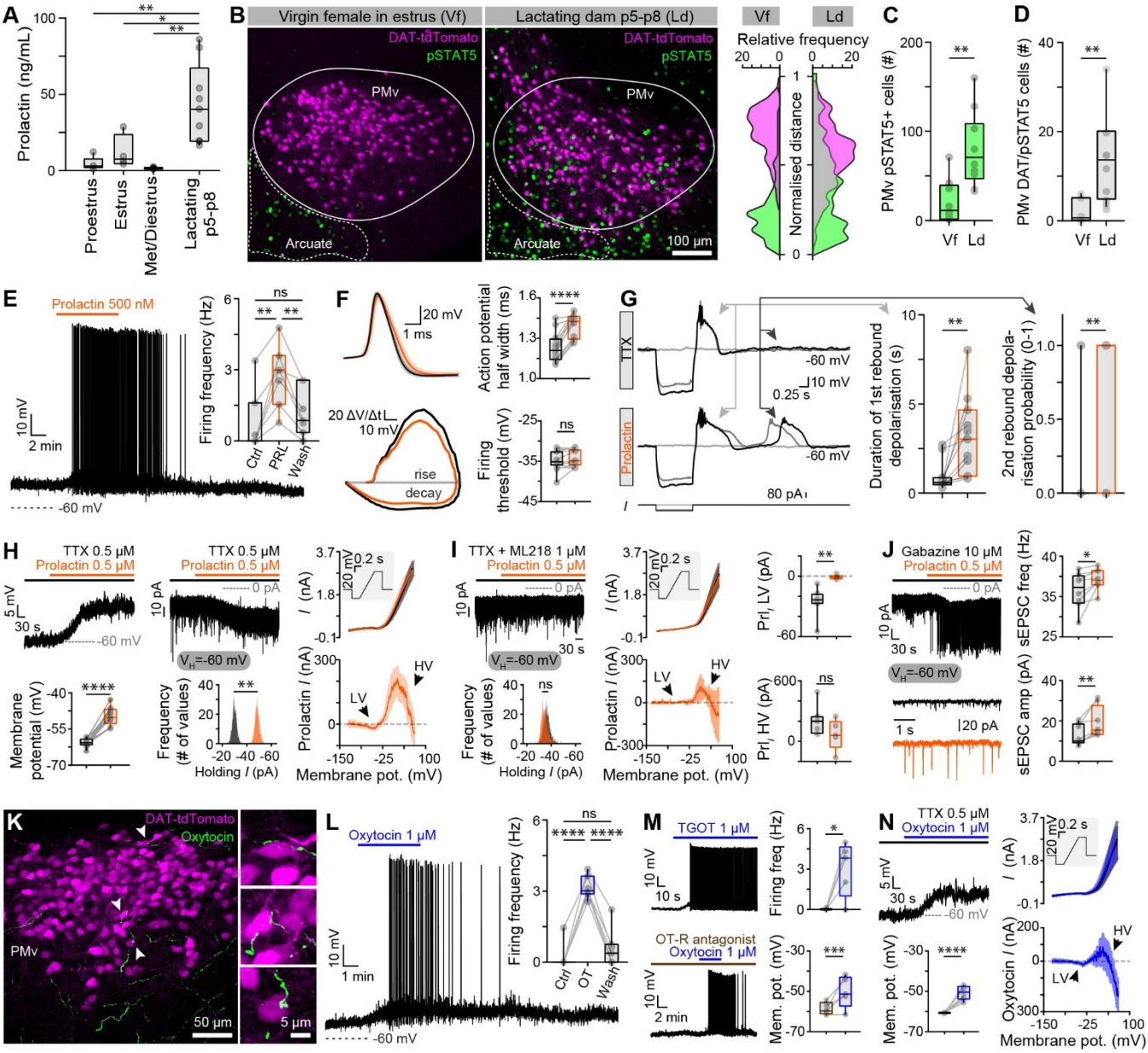

Figure 3. Maternal hormones activate PMv^{DAT} neurons.

(A) Serum prolactin levels in virgin females across the estrous cycle (proestrus, estrus, met-/diestrus) *vs* lactating dams (n = 4-9 mice per group, ordinary one-way ANOVA, p = 0.0007).

(B) Confocal images of pSTAT5 immunoreactivity in PMv, in virgin females in estrus *vs* lactating dams (left). Overlap of pSTAT5 and DAT-tdTomato fluorescence along the Y axis, with 0 being the most ventral point of the confocal image and 1 the most dorsal (right).

(C) Quantification of pSTAT5 immunoreactive cells in the PMv of virgin females in estrus *vs* lactating dams (n = 10 sections per group, 5 mice per group, 2 sections per mouse, two-tailed unpaired t-test, p = 0.0011).

897 (D) Quantification of DAT-tdTomato colocalizing pSTAT5 immunoreactive cells in the PMv of virgin
898 females in estrus *vs* lactating dams (n = 10 sections per group, 5 mice per group, 2 sections per
899 mouse, two-tailed unpaired t-test, p = 0.0015).
900 (E) Application of prolactin leads to a reversible depolarisation of PMv^{DAT} neurons (n = 7 cells from 5
901 mice, RM one-way ANOVA, p = 0.0016).
902 (F) Prolactin induced changes in the action potential waveform of PMv^{DAT} neurons (left). Quantification
903 of action potential (AP) half-width and firing threshold in control (black) *vs* prolactin (orange, n = 15
904 action potentials in control *vs* bath application of prolactin per cell, 7 cells from 5 mice, two-tailed
905 paired t-test).
906 (G) (left) Comparison of post-inhibitory rebound bouts in control (TTX) *vs* prolactin application (TTX +
907 prolactin). Black traces represent the hyperpolarization induced by the highest absolute amplitude
908 negative current pulse, with the effect of a smaller amplitude pulse illustrated in dark gray and the
909 absence of any pulse in light gray. (middle) Quantification of the 1st post-inhibitory rebound in control
910 (black) *vs* prolactin (orange, n = 11 cells per group collected from 6 mice, two-tailed paired t-test, p =
911 0.0098). (right) Quantification of a 2nd post-inhibitory rebound probability in control (black) *vs* prolactin
912 (orange, n = 11 cells per group collected from 6 mice, two-tailed paired t-test, p = 0.0061).
913 (H) Identification of a prolactin-induced postsynaptic depolarisation on PMv^{DAT} cells in current clamp
914 (left, n=13 cells per group collected from 8 mice, two-tailed paired t-test, p < 0.0001) and voltage
915 clamp (middle, n = 5 cells per group collected from 5 mice, two-tailed paired t-test, p = 0.0078).
916 Characterisation of the prolactin-induced current across the membrane voltage spectrum in PMv^{DAT}
917 neurons, with a low- and high-voltage component (right, n = 7 cells collected from 4 mice).
918 (I) Application of the selective T-type Ca^{2+} current blocker, ML218, blocks the low-voltage component
919 of the prolactin-induced current (Prl_I). Application of prolactin does not induce an inward current in
920 PMv^{DAT} neurons pre-exposed to ML218 (left, n = 6 cells per group collected from 4 mice, two-tailed
921 paired t-test, p = 0.5129). In the presence of ML218 the prolactin-induced current is composed only
922 of a high-voltage component (middle, n = 6 cells collected from 4 mice). Comparison of the low- (right,
923 n=6-7 cells per group, two-tailed unpaired t-test, p = 0.0042) and high-voltage (right, n=6-7 cells per
924 group, two-tailed unpaired t-test, p = 0.1384) components of the prolactin-induced current in the
925 absence *vs* presence of ML218.
926 (J) Electrophysiology recordings of spontaneous excitatory postsynaptic currents during application
927 of gabazine (to block fast inhibitory synaptic transmission) and of Prl (n = 8 cells collected from 4
928 mice).
929 (K) Oxytocin-immunoreactive fibers forming close appositions to PMv^{DAT} neurons (n = 5 mice).
930 (L) Oxytocin leads to a reversible depolarisation of PMv^{DAT} neurons (n = 7 cells per group, collected
931 from 5 mice, RM one-way ANOVA, p < 0.0001).
932 (M) Application of the selective oxytocin receptor agonist, TGOT, leads to depolarisation of PMv^{DAT}
933 neurons (top, n = 5 cells per group, collected from 5 mice, two-tailed paired t-test, p = 0.0274). Under

934 oxytocin receptor blockade, the oxytocin-induced depolarisation of PMv^{DAT} neurons persists (bottom,
935 n = 5 cells per group, collected from 5 mice, two-tailed paired t-test, $p = 0.0008$).
936 (N) Identification of an oxytocin-induced postsynaptic depolarisation on PMv^{DAT} cells in current clamp
937 (left, n=8 cells per group collected from 4 mice, two-tailed paired t-test, $p < 0.0001$). Characterisation
938 of the oxytocin-induced current across the membrane voltage spectrum in PMv^{DAT} neurons, with a
939 low- and high-voltage component (right, n = 8 cells collected from 4 mice).
940 See also Table S1.

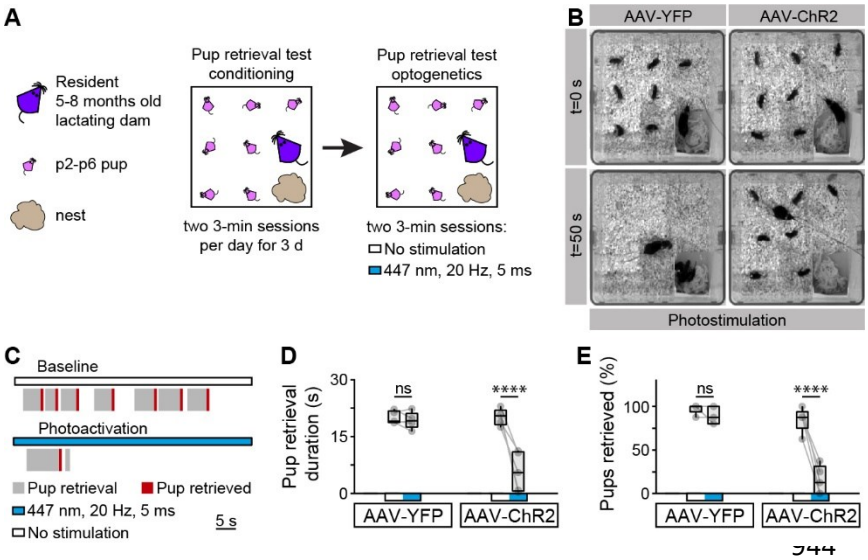

Figure 4. Activation of PMv^{DAT} neurons suppresses non-aggression-related behavioural programs.

(A) Schematic of the experimental design used to perform ChR2 PMv^{DAT} neuron photoactivation during the pup retrieval test.

(B) Images from two photostimulation trials at the start (0 s) and 50 s *post*-trial initiation, with lactating dams expressing eYFP (left) and ChR2 (right) in PMv^{DAT} neurons.

(C) Sample behaviour raster plots of two sequential trials without and with photostimulation in a ChR2-expressing lactating dam during the pup retrieval test.

(D) Pup retrieval duration with and without photostimulation in lactating dams injected with eYFP or ChR2, during the pup retrieval test (n = 5 mice per group, ordinary one-way ANOVA, $p < 0.0001$).

(E) Percentage of pups retrieved with and without photostimulation in lactating dams injected with eYFP or ChR2, during the pup retrieval test (n = 5 mice per group, ordinary one-way ANOVA, $p < 0.0001$).

See also Table S1.

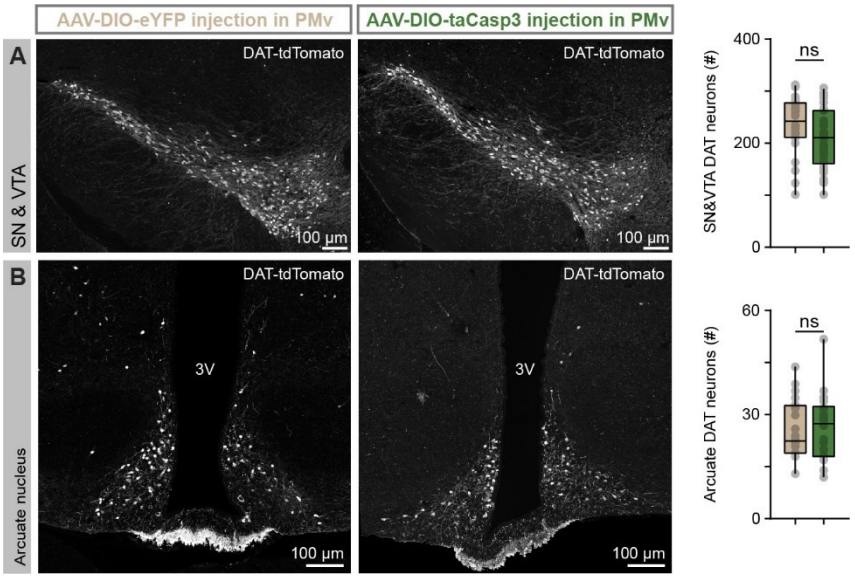

Figure S1. Injection of AAV-flex-taCasp3 in the PMv of DAT-Cre animals does not extend along the rostrocaudal axis, leaving the midbrain and arcuate nucleus dopamine neurons intact, related to Figure 2.

(A) Confocal image of an eYFP- (left) *vs* taCasp3- (middle) PMv injected sample sections of midbrain (substantia nigra, SN, and ventral tegmental area, VTA) DAT-tdTomato neurons, and quantification of cell number per section (n = 24-26 sections per group, duplicates from 12-13 mice per group, two-tailed unpaired t-test, p = 0.1141).

(B) Confocal image of an eYFP- (left) *vs* taCasp3- (middle) PMv injected sample sections of arcuate DAT-tdTomato neurons, and quantification of cell number per section (n = 24-26 sections per group, duplicates from 12-13 mice per group, two-tailed unpaired t-test, p = 0.5650). 3V, third ventricle. See also Table S1.

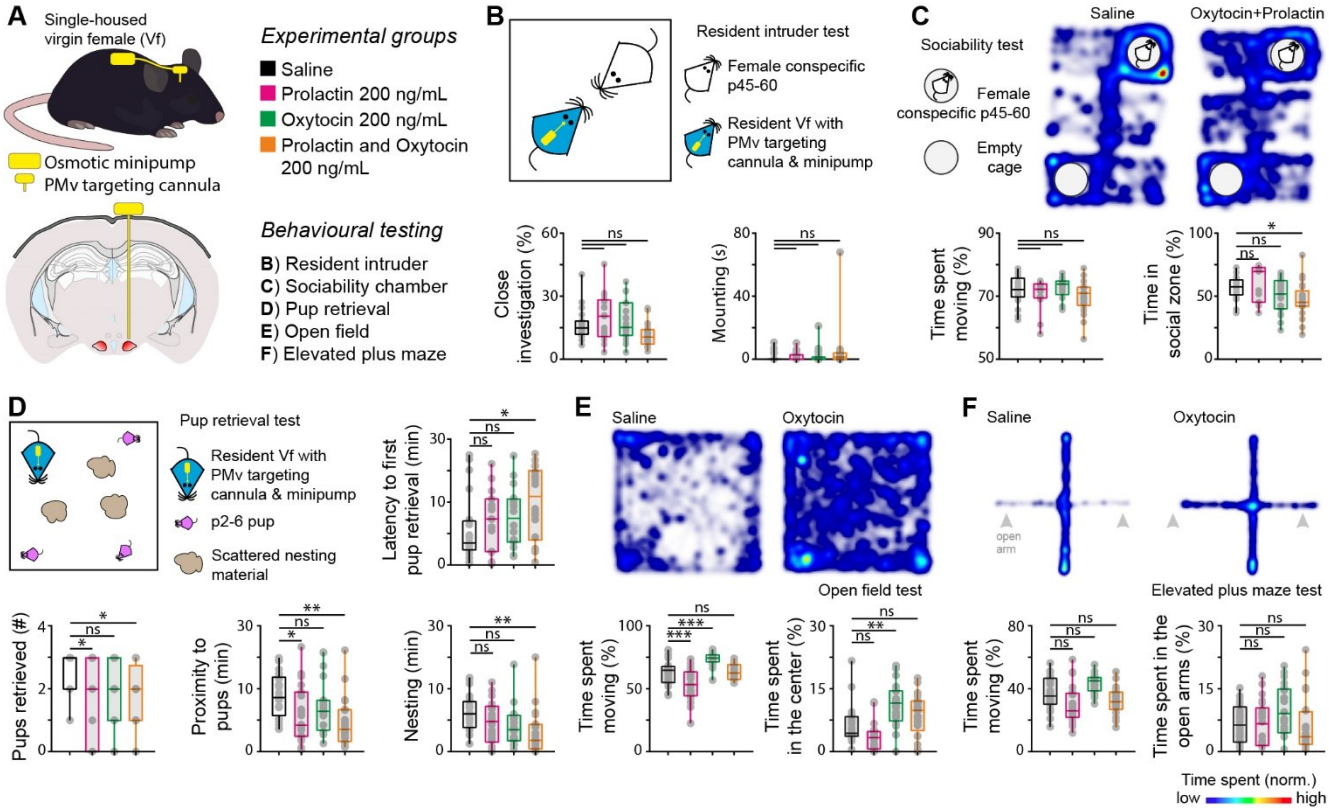

Figure S2. Chronic administration of maternal hormones in the PMv is not sufficient to evoke aggression in virgin females, related to Figure 3.

(A) Schematic of the experimental design followed to infuse maternal hormones into the PMv parenchyma via cannulas for a period of 28 days, and perform a panel of behavioural tests.
(B) Design and quantification of social behaviours in the RI test, with implanted resident adult virgin females *vs* juvenile virgin female intruders. No changes in close investigation or mounting duration were recorded (n = 21-24 trials per group, triplicates from 7-8 mice per group, RM one-way ANOVA). No episodes of aggression occurred in any of the groups.
(C) Design and results from the sociability test, where implanted adult virgin female mice can choose between an empty chamber and one with a juvenile virgin female conspecific present. (n = 13-24 trials per group, duplicates or triplicates from 7-8 mice per group, ordinary one-way ANOVA).
(D) Design and results from the pup retrieval test, with implanted adult virgin female mice (n = 21-24 trials per group, triplicates from 7-8 mice per group, ordinary one-way ANOVA).
(E) Results from the open field test, with implanted adult virgin female mice (n = 21-24 trials per group, triplicates from 7-8 mice per group, ordinary one-way ANOVA).
(F) Results from the elevated plus maze test, with implanted adult virgin female mice (n = 21-24 trials per group, triplicates from 7-8 mice per group, ordinary one-way ANOVA). See also Table S1.

995 Table S1

Figures	Test	n (per group)	KW statistic or t values	df	p value	Comparisons	Adjusted p value	p value summary
Figure 1B, left – attack duration (%)	RM one-way ANOVA with Kruskal-Wallis post-hoc test	12	KW statistic = 18.18	11	0.0001	day 1 *vs*. day 2	0.0051	**
						day 1 *vs*. day 3	0.0001	***
						day 2 *vs*. day 3	>0.9999	ns
Figure 1B, right – attack latency (s)	RM one-way ANOVA with Kruskal-Wallis post-hoc test	12	KW statistic = 7.182	11	0.0276	day 1 *vs*. day 2	0.2988	ns
						day 1 *vs*. day 3	0.0238	*
						day 2 *vs*. day 3	0.9411	ns
Figure 1D, c-Fos cells (#)	Two-tailed unpaired t-test	10-12	t = 9.661	20	< 0.0001	c-Fos in PMv without *vs.* with intruder	N/A	****
Figure 1D, DAT/c-Fos cells (#)			t = 11.72			DAT/c-Fos colocalization without *vs.* with intruder	N/A	****
Figure 1H, firing frequency (Hz)	Two-tailed unpaired t-test	21-53	t = 4.540	72	< 0.0001	virgin *vs.* lactating	N/A	****

996

997

Figures	Test	n (per group)	F or t values	df	p value	Comparisons	Adjusted p value	p value summary
Figure 2D, attack duration (s)	Ordinary one-way ANOVA with uncorrected Fisher's LSD test as multiple comparisons test	5-9	$F_{(7, 48)} = 11.55$	7	< 0.0001	AAV-eYFP dam, against adult virgin male intruder – baseline *vs.* photostimulation	> 0.9999	ns
						AAV-eYFP dam, against adult virgin female intruder – baseline *vs.* photostimulation	> 0.9999	ns
						AAV-ChR2 dam, against adult virgin male intruder – baseline *vs.* photostimulation	> 0.9999	ns
						AAV-ChR2 dam, against adult virgin female intruder – baseline *vs.* photostimulation	< 0.0001	****
Figure 2E, attack latency (s)	Ordinary one-way ANOVA with uncorrected Fisher's LSD test as multiple comparisons test	5-9	$F_{(7, 48)} = 3.732$	7	0.0027	AAV-eYFP dam, against adult virgin male intruder – baseline *vs.* photostimulation	0.7149	ns
						AAV-eYFP dam, against adult virgin female intruder – baseline *vs.* photostimulation	0.9468	ns
						AAV-ChR2 dam, against adult virgin male intruder – baseline *vs.* photostimulation	0.1043	ns
						AAV-ChR2 dam, against adult virgin female intruder – baseline *vs.* photostimulation	0.0266	*

Figures	Test	n (per group)	F or t values	df	p value	Comparisons	Adjusted p value	p value summary
Figure 2I, left attack duration/trial (s)	Two-tailed paired t-test	8	t = 9.280	7	< 0.0001	AAV-ChR2 dam, against a juvenile virgin female intruder – baseline *vs.* photostimulation	N/A	****
Figure 2I, middle attack bout (s)	Two-tailed paired t-test	8	t = 5.356	7	0.0011	AAV-ChR2 dam, against a juvenile virgin female intruder – baseline *vs.* photostimulation	N/A	**
Figure 2I, right attack frequency/trial (#)	Two-tailed paired t-test	8	t = 3.752	7	0.0071	AAV-ChR2 dam, against a juvenile virgin female intruder – baseline *vs.* photostimulation	N/A	**
Figure 2J, latency to first attack following a photoinhibition episode (s)	Two-tailed paired t-test	8	t = 3.300	7	0.0131	AAV-ChR2 dam, against a juvenile virgin female intruder – baseline *vs.* photostimulation	N/A	*
Figure 2N, left attack duration (%)	Two-tailed unpaired t-test	34	t = 8.827	54	< 0.0001	against a juvenile virgin female intruder – eYFP *vs.* taCasp3 injected lactating dams	N/A	****
Figure 2N, middle attack frequency (#)	Two-tailed unpaired t-test	34	t = 5.348	66	< 0.0001	against a juvenile virgin female intruder – eYFP *vs.* taCasp3 injected lactating dams	N/A	****
Figure 2N, right latency to first attack (min)	Two-tailed unpaired t-test	34	t = 6.506	41	< 0.0001	against a juvenile virgin female intruder – eYFP *vs.* taCasp3 injected lactating dams	N/A	****
Figure 2O, PMv^{DAT} neurons (#)	Two-tailed unpaired t-test	24	t = 22.78	48	< 0.0001	eYFP *vs.* taCasp3 injected lactating dams	N/A	****

Figures	Test	n (per group)	F or t values	df	p value	Comparisons	Adjusted p value	p value summary
Figure 3A, Serum Prolactin (ng/mL)	Ordinary one-way ANOVA with Dunnett's multiple comparisons test	4-9	$F_{(3, 19)} = 8.797$	3	0.0007	proestrus *vs.* lactating	0.0022	**
						estrus *vs.* lactating	0.0199	*
						met-/diestrus *vs.* lactating	0.0011	**
Figure 3C, pSTAT5 cells in PMv (#)	Two-tailed unpaired t-test	10	t = 3.878	18	0.0011	Virgin in estrus *vs.* lactating	N/A	**
Figure 3D, PMv^{DAT}/pSTAT5 cell colocalization (#)	Two-tailed unpaired t-test	10	t = 3.737	18	0.0015	Virgin in estrus *vs.* lactating	N/A	**
Figure 3E, firing frequency (Hz)	RM one-way ANOVA with Bonferroni's multiple comparisons test	7	$F_{(1.723, 10.34)} = 13.73$	6	0.0016	control *vs.* prolactin	0.0069	**
						control *vs.* wash	> 0.9999	ns
						prolactin *vs.* wash	0.0097	**
Figure 3F, action potential half width (ms)	Two-tailed paired t-test	15	t = 8.847	14	< 0.0001	control *vs.* prolactin	N/A	****
Figure 3F, action potential firing threshold (mV)	Two-tailed paired t-test	15	t = 1.926	14	0.0746	control *vs.* prolactin	N/A	ns
Figure 3G, duration of 1st rebound depolarisation (s)	Two-tailed paired t-test	11	t = 3.183	10	0.0098	control *vs.* prolactin	N/A	**
Figure 3G, 2nd rebound depolarisation probability	Two-tailed paired t-test	11	t = 3.464	10	0.0061	control *vs.* prolactin	N/A	**
Figure 3H, left membrane potential (mV)	Two-tailed paired t-test	13	t = 9.753	12	< 0.0001	control *vs.* prolactin	N/A	****
Figure 3H, middle Holding I (pA)	Two-tailed paired t-test	5	t = 4.941	4	0.0078	control *vs.* prolactin	N/A	**
Figure 3I, left Holding I (pA)	Two-tailed paired t-test	6	t = 0.7040	5	0.5129	control *vs.* prolactin	N/A	ns

Figure 3I, top right Prl/ LV(pA)	Two-tailed unpaired t-test	5-7	t = 3.685	10	0.0042	control *vs.* prolactin	N/A	**
Figure 3I, bottom right Prl/ LV(pA)	Two-tailed unpaired t-test	5-7	t = 1.611	10	0.1384	control *vs.* prolactin	N/A	ns
Figure 3J, top right sEPSC frequency (Hz)	Two-tailed paired t-test	8	t = 3.609	7	0.014	control *vs.* prolactin	N/A	*
Figure 3J, bottom right sEPSC amplitude (pA)	Two-tailed paired t-test	8	t = 4.069	7	0.0048	control *vs.* prolactin	N/A	**
Figure 3L, firing frequency (Hz)	RM one-way ANOVA with Bonferroni's multiple comparisons test	7	$F_{(1.114, 6.682)} = 75.40$	6	< 0.0001	control *vs.* oxytocin	< 0.0001	****
						control *vs.* wash	> 0.9999	ns
						oxytocin *vs.* wash	< 0.0001	****
Figure 3M, top firing frequency (Hz)	Two-tailed paired t-test	5	t = 3.393	4	0.0274	control *vs.* TGOT	N/A	*
Figure 3M, bottom membrane pot. (mV)	Two-tailed paired t-test	5	t = 9.253	4	0.0008	control *vs.* TGOT	N/A	***
Figure 3N, left membrane pot. (mV)	Two-tailed paired t-test	8	t = 8.040	7	< 0.0001	control *vs.* TGOT	N/A	****

1000

Figures	Test	n (per group)	F or t values	df	p value	Comparisons	Adjusted p value	p value summary
Figure 4D, pup retrieval duration (s)	Ordinary one-way ANOVA with Bonferroni's multiple comparisons test	5	$F_{(3, 16)} = 25.59$	3	< 0.0001	AAV-eYFP dam – baseline *vs.* photostimulation	> 0.9999	ns
						AAV-ChR2 dam – baseline *vs.* photostimulation	< 0.0001	****
Figure 4E, pup retrieved (%)	Ordinary one-way ANOVA with Bonferroni's multiple comparisons test	5	$F_{(3, 16)} = 49.80$	3	< 0.0001	AAV-eYFP dam – baseline *vs.* photostimulation	> 0.9999	ns
						AAV-ChR2 dam – baseline *vs.* photostimulation	< 0.0001	****
Figure S1A, SN&VTA DAT neurons (#)	Two-tailed unpaired t-test	24-26	t = 1.609	48	0.1141	eYFP *vs.* taCasp3 injected lactating dams	N/A	ns
Figure S1B, arcuate DAT neurons (#)	Two-tailed unpaired t-test	24-26	t = 0.5794	48	0.5650	eYFP *vs.* taCasp3 injected lactating dams	N/A	ns
Figure S2B, close investigation (%)	RM one-way ANOVA with Bonferroni's multiple comparisons test	21-24	$F_{(3, 83)} = 3.760$	3	0.0138	saline *vs.* prolactin (Prl)	0.8239	ns
						saline *vs.* oxytocin (OT)	> 0.9999	ns
						saline *vs.* Prl & OT	0.1259	ns
Figure S2B, mounting (s)	RM one-way ANOVA with Bonferroni's multiple comparisons test	21-24	$F_{(3, 83)} = 0.9736$	3	0.4092	saline *vs.* prolactin (Prl)	> 0.9999	ns
						saline *vs.* oxytocin (OT)	> 0.9999	ns
						saline *vs.* Prl & OT	0.3291	ns
Figure S2C, time spent moving (%)	RM one-way ANOVA with Bonferroni's multiple comparisons test	13-24	$F_{(3, 75)} = 1.698$	3	0.1747	saline *vs.* prolactin (Prl)	> 0.9999	ns
						saline *vs.* oxytocin (OT)	> 0.9999	ns
						saline *vs.* Prl & OT	0.4069	ns
Figure S2C, time in social zone (%)	RM one-way ANOVA with Bonferroni's multiple comparisons test	13-24	$F_{(3, 75)} = 3.953$	3	0.0114	saline *vs.* prolactin (Prl)	> 0.9999	ns
						saline *vs.* oxytocin (OT)	0.2401	ns
						saline *vs.* Prl & OT	0.0346	*

Figures	Test	n (per group)	F or t values	df	p value	Comparisons	Adjusted p value	p value summary
Figure S2D, latency to first pup retrieval (min)	RM one-way ANOVA with Bonferroni's multiple comparisons test	15-20	$F_{(3, 65)} = 2.150$	3	0.1025	saline *vs.* prolactin (Prl)	> 0.9999	ns
						saline *vs.* oxytocin (OT)	0.8639	ns
						saline *vs.* Prl & OT	0.0418	*
Figure S2D, pups retrieved (#)	RM one-way ANOVA with Bonferroni's multiple comparisons test	20-24	$F_{(3, 82)} = 3.452$	3	0.0202	saline *vs.* prolactin (Prl)	0.0124	*
						saline *vs.* oxytocin (OT)	0.8639	ns
						saline *vs.* Prl & OT	0.0432	*
Figure S2D, proximity to pups (min)	RM one-way ANOVA with Bonferroni's multiple comparisons test	20-24	$F_{(3, 82)} = 4.716$	3	0.0044	saline *vs.* prolactin (Prl)	0.0330	*
						saline *vs.* oxytocin (OT)	0.3891	ns
						saline *vs.* Prl & OT	0.0017	**
Figure S2D, nesting (min)	RM one-way ANOVA with Bonferroni's multiple comparisons test	20-24	$F_{(3, 82)} = 3.819$	3	0.0129	saline *vs.* prolactin (Prl)	0.2276	ns
						saline *vs.* oxytocin (OT)	0.0669	ns
						saline *vs.* Prl & OT	0.0051	**
Figure S2E, time spent moving (%)	RM one-way ANOVA with Bonferroni's multiple comparisons test	21-24	$F_{(3, 83)} = 18.17$	3	< 0.0001	saline *vs.* prolactin (Prl)	0.0007	***
						saline *vs.* oxytocin (OT)	0.0009	***
						saline *vs.* Prl & OT	> 0.9999	ns
Figure S2E, time spent in the center (%)	RM one-way ANOVA with Bonferroni's multiple comparisons test	21-24	$F_{(3, 83)} = 10.59$	3	< 0.0001	saline *vs* prolactin (Prl)	0.1397	ns
						saline *vs.* oxytocin (OT)	0.0025	**
						saline *vs.* Prl & OT	0.1915	ns
Figure S2F, time spent moving (%)	RM one-way ANOVA with Bonferroni's multiple comparisons test	21-24	$F_{(3, 83)} = 7.991$	3	< 0.0001	saline *vs.* prolactin (Prl)	0.0697	ns
						saline *vs.* oxytocin (OT)	0.0578	ns
						saline *vs.* Prl & OT	0.4917	ns

Figures	Test	n (per group)	F or t values	df	p value	Comparisons	Adjusted p value	p value summary
Figure S2F, time spent in the open arms (%)	RM one-way ANOVA with Bonferroni's multiple comparisons test	21-24	$F_{(3, 83)} = 2.163$	3	0.0985	saline *vs.* prolactin (Prl)	> 0.9999	ns
						saline *vs.* oxytocin (OT)	0.1189	ns
						saline *vs.* Prl & OT	> 0.9999	ns

1002